

UC San Diego

UC San Diego Electronic Theses and Dissertations

Title

Environmental Bloom of Lingulodinium polyedrum in Southern California: Potential Health Risks

Permalink

<https://escholarship.org/uc/item/3zb9b1rp>

Author

Lee, John

Publication Date

2015

Peer reviewed|Thesis/dissertation

UNIVERSITY OF CALIFORNIA, SAN DIEGO

Environmental Bloom of *Lingulodinium polyedrum* in Southern California: Potential
Health Risks

A Thesis submitted in partial satisfaction of the requirements for the degree Master of
Science

in

Chemistry

by

John Lee

Committee in charge:

Lena Gerwick, Chair
William H. Gerwick
Simpson Joseph
Emmanuel Theodorakis

2015

Copyright

John Lee, 2015

All rights reserved.

The Thesis of John Lee is approved, and it is acceptable in quality and form for publication on microfilm and electronically:

Chair

Table of Contents

Signature Page.....	iii
Table of Contents.....	iv
List of Figures.....	vi
Acknowledgements.....	viii
Abstract of the Thesis.....	ix
Chapter One	
Rising Concern Regarding Harmful Algal Blooms and <i>L. polyedrum</i> Blooms.....	1
Chapter Two	
Methods.....	5
2.1 Extraction of <i>L. polyedrum</i> cell culture.....	6
2.2 Vacuum-liquid Chromatography Fractionation of <i>L. polyedrum</i> cell culture extraction.....	7
2.3 Extraction of <i>L. polyedrum</i> cell culture for yessotoxin-like metabolites.....	8
2.4 Nitric Oxide Inflammatory Response <i>in Vitro</i> assay.....	9
2.5 Cell Proliferation <i>in Vitro</i> assay.....	10
2.6 Liquid Chromatography-Mass Spectrometry Analysis.....	10
2.7 MS/MS Molecular Networking.....	11
2.8 Isolation of Digalactosyldiacylglycerol (20:5/18:5) and Monogalactosyldiacylglycerol (20:5/18:5).....	11
2.9 1D NMR Analysis of <i>L. polyedrum</i> Fractions.....	12
Chapter Three	
Assay-guided Extraction of <i>L. polyedrum</i> Cell Culture.....	13
3.1 <i>L. polyedrum</i> Cell Culture Extraction.....	14
3.2 Nitric Oxide Inflammatory Response and Cell Proliferation Assay of <i>L. polyedrum</i> Extraction.....	15
Chapter Four	
Identification and Isolation of Digalactosryldiacylglycerol (20:5/18:5) and Monogalactosyldiacylglycerol (20:5/18:5)	25

4.1 Liquid Chromatography-Mass Spectrometry Analysis of Active <i>L. polyedrum</i> Fractions.....	26
4.2 Molecular Networking of <i>L. polyedrum</i> Extraction.....	26
4.3 1D Proton NMR Analysis of Active <i>L. polyedrum</i> Fractions.....	27
4.4 Determination of Monogalactosyldiacylglycerol (20:5/18:5) as the Molecule of Interest.....	28
4.5 High-performance Liquid Chromatography Isolation of Digalactosyldiacylglycerol (20:5/18:5) and Monogalactosyldiacylglycerol (20:5/18:5).....	29
4.6 Nitric Oxide Inflammatory Response and Cell Proliferation Assay of Digalactosyldiacylglycerol (20:5/18:5) and Monogalactosyldiacylglycerol (20:5/18:5)..	29
Chapter Five	
Extraction of <i>L. polyedrum</i> cell culture for Yessotoxin-like Metabolites.....	40
5.1 Yessotoxin-like Metabolite Extraction of <i>L. polyedrum</i> Cell Cultures.....	41
Chapter Six	
Discussion and Conclusions.....	44
6.1 Discussion.....	45
6.2 Conclusions.....	48
References.....	51

List of Figures

Figure 2.1. Vacuum-liquid Chromatography Fractionation of <i>L. polyedrum</i> cell extract.....	7
Figure 2.2. Vacuum-liquid Chromatography Fractionation of <i>L. polyedrum</i> cell media extract.....	8
Figure 3.1. Vacuum-liquid Chromatography Fractionation of <i>L. polyedrum</i> cell extract.....	16
Figure 3.2. Vacuum-liquid Chromatography Fractionation of <i>L. polyedrum</i> cell media extract.....	17
Figure 3.3. <i>L. polyedrum</i> cell fraction Inflammation and Cytotoxicity Assay at 30 $\mu\text{g/mL}$	18
Figure 3.4. <i>L. polyedrum</i> cell fractions tested. Increase in NO production and Cytotoxicity at 10 $\mu\text{g/mL}$	19
Figure 3.5. <i>L. polyedrum</i> cell fraction Inflammation and Cytotoxicity Assay at 3 $\mu\text{g/mL}$	20
Figure 3.6. <i>L. polyedrum</i> cell fraction Inflammation and Cytotoxicity Assay at 1 $\mu\text{g/mL}$	21
Figure 3.7. <i>L. polyedrum</i> cell fraction Inflammation and Cytotoxicity Assay at 0.3 $\mu\text{g/mL}$	22
Figure 3.8. <i>L. polyedrum</i> cell fraction Inflammation and Cytotoxicity Assay at 0.1 $\mu\text{g/mL}$	23
Figure 4.1. Liquid Chromatography-Mass Spectrometry Analysis of Fraction E.....	30
Figure 4.2. Liquid Chromatography-Mass Spectrometry Analysis of Fraction F.....	31
Figure 4.3. Liquid Chromatography-Mass Spectrometry Analysis of Fraction G.....	32
Figure 4.4. Molecular Network of <i>L. polyedrum</i> Cell and Media Extract Fractions.....	33
Figure 4.5. Molecular Network of <i>L. polyedrum</i> Cell and Media Extract Fractions Excluding Library Ions.....	34
Figure 4.6. 1D Proton NMR Analysis of Fraction F.....	35

Figure 4.7. 1D Proton NMR Prediction of Proposed Monogalactosyldiaclyglycerol (20:5/18:5) Structure.....	36
Figure 4.8. Chemical Structure of Digalactosyldiaclyglycerol (20:5/18:5).....	37
Figure 4.9. Chemical Structure of Monogalactosyldiaclyglycerol (20:5/18:5).....	37
Figure 4.10. Digalactosyldiaclyglycerol (20:5/18:5) Inflammation and Cytotoxicity Assay.....	38
Figure 4.11. Monogalactosyldiaclyglycerol (20:5/18:5) Inflammation and Cytotoxicity Assay.....	39
Figure 5.1. Liquid Chromatography-Mass Spectrometry Analysis of Yessotoxin Standard.....	43
Figure 6.1. Liquid Chromatography-Mass Spectrometry Analysis of 17.59 minute peak in Fraction G.....	49
Figure 6.2. Chemical Structure of Monogalactosyldiaclyglycerol (18:5/18:5).....	49
Figure 6.3. Liquid Chromatography-Mass Spectrometry Analysis of 18.90 minute peak in Fraction G.....	50
Figure 6.4. Chemical Structure of Monogalactosyldiaclyglycerol (20:5/18:4).....	50

Acknowledgements

I would firstly want to thank Dr. Lena and Dr. Bill Gerwick for providing me the opportunity to become a part of their lab group as first a volunteer and later a Masters student. I have learned more than I had ever anticipated under their guidance and mentorship and am indebted to them for the knowledge and skills I have acquired. I would also like to thank Dr. Matt Bertin for his assistance and guidance with a significant portion of the chemistry work presented here. I would also like to thank Dr. Sam Mascuch for her tutelage and assistance in the care of the tissue cultures used by the lab as well as Dr. Evgenia Glukhov for her tireless work in the Gerwick Lab. Of course, I have to thank all members of the Gerwick Lab, past and present, for making my time in the group a memorable and amazing experience. I would also like to thank Dr. Michael Latz who graciously provided us with the *L. polyedrum* cultures which were essential to this work as well as Dr. Theresa Gaasterland and Melissa Carter for sharing their knowledge which was key to this thesis. Lastly, I would like to thank NIEHS for providing the grant (ES024105) under which this work was completed.

ABSTRACT OF THESIS

Environmental Bloom of *Lingulodinium polyedrum* in Southern California: Potential Health Risks

by

John Lee

Master of Science in Chemistry

University of California, San Diego, 2015

Lena Gerwick, Chair

Harmful algal blooms (HABs) have been documented to harbor algae capable of producing toxins harmful to both humans and marine life. *Lingulodinium polyedrum*, the major dinoflagellate species in the recent algal blooms in southern California in 2011 and 2013, has been shown to induce allergic responses in humans exposed to the bloom. The

chemical natures of the compounds produced by *L. polyedrum* which induce this response are as of yet unknown. This study had the goal of determining whether *L. polyedrum* contains any pro-inflammatory compounds and to discern whether these compounds could induce an allergic reaction. Bioassay guided fractionation and chemical separation of cultured *L. polyedrum* has led to the isolation of a glycolipid produced by *L. polyedrum*, monogalactosyldiacylglycerol (20:5/18:5). Evaluation of the pro-inflammatory capacity of this glycolipid revealed that this glycolipid does not induce a pro-inflammatory response.

Chapter One

Introduction:

Rising Concern Regarding Harmful Algal Blooms and *L. polyedrum* Blooms

Harmful Algal Blooms (HABs) have become a growing global concern, causing problems in the environment through their detrimental effects on other aquatic life and ecosystems, threats to public health with a number of blooms harboring toxin producing species, as well as difficulties commercially with blooms affecting the quality of harvested seafood. Harmful Algal Blooms are also becoming a growing concern as incidences of blooms have been increasing in recent years, the discovery of new toxic species of algae, as well as previously nontoxic species having been found capable of producing toxins (Hallegraeff, G.M. 1993)(Mclean, T.I. and Sinclair, G.A. 2012).

Before delving into the specifics of these issues, it is necessary to first define what constitutes a Harmful Algal Bloom and what designates these phenomena as harmful. Algae is a broad term used to describe a number of phyla rather than an actual taxonomic designation as its use predates genomic classification. Algae are generally defined as mainly aquatic, photosynthetic organisms which lack vascular systems and can be unicellular or multicellular (Huisman, J.M. et al 2007). A few examples of which are considered algae are the prokaryotic cyanobacteria, heterokontophyta, which consists largely of diatoms, and dinoflagellates. An algal bloom occurs when the population count of a species of algae significantly increases in number due to an increase rate of growth, often as a result of a sudden increase in available nutrients, though specifics differ from species to species (Smayda, T.J. and Reynolds, C.S. 2001). This is a global phenomenon, occurring in both fresh water and marine environments. Often when a tide occurs, the high density of cells produces a visible color change in the water which leads to the common name for blooms, “red tide.” However, the color of a bloom depends on the

color of the pigment(s) of the dominant species causing the bloom which may be red, green, or brown, to name a few.

Algal blooms are often associated with negative connotations, and, although not all algal blooms are harmful with many blooms occurring naturally and providing a source of food for many aquatic organisms, there are a number of blooms which have caused a great deal of concern regarding their adverse effects . It is these blooms that have become a focal point of research in recent years.

There are a number of ways by which algal blooms can be considered harmful. Some blooms cause problems indirectly due to increased growth of a population, leading to high consumption of resources which can also lead to detrimental effects due to high concentrations of waste products (Dagg, M.J. 2007)(Rabalais, N.N. 2002). More directly, blooms can also damage other organisms due to their physical characteristics, which some diatoms are known to cause, while other blooms contain species which secrete chemicals which can disrupt their immediate environment(Legrand, C. 2003), such as ammonium (Okaichi, T. 1976). Though these are significantly harmful effects of some algal blooms, the main focus of much harmful algal bloom research concerns itself with algal blooms species which produce toxins.

The main focus of this research is to examine the *Lingulodinium polyedrum* bloom along the coast of La Jolla near Scripps Institution of Oceanography. Blooms of this dinoflagellate have occurred along the California coast somewhat regularly for many years with the most recent blooms occurring in 2011 and 2013 (Moorthi, S.D. et al 2006). *Lingulodinium polyedrum* is a photosynthetic bloom forming species capable of bioluminescence as a stress response which results in bioluminescent blooms. *L.*

polyedrum is a known producer of the yessotoxins, disulfated polyethers which had previously been considered a toxin which induces Diarrhetic Shellfish Poisoning (DSP); however, the yessotoxins have been shown to not induce diarrhea, are incapable of protein phosphatase inhibition and are no longer considered a DSP toxin. However, the yessotoxins have been shown to possess cytotoxic effects, specifically through damaging Purkinje cells in the cerebellar cortex of mice (Franchini, A. 2004) and caspase activation-induced cell death in HeLa cells (Malaguti, C. et al 2002). However, anecdotal accounts of allergic responses, for example severe flushing of the skin, difficulty breathing and urticaria, have been reported from people visiting the beach during these blooms.

To address potential pro-inflammatory effects, the work presented here aims to assess the pro-inflammatory capabilities of *L. polyedrum* using assay-guided fractionation and isolation of compounds produced by this dinoflagellate. *L. polyedrum* cell mass was first processed through filtration and fractionation and subsequently tested in an *in vitro* inflammatory response assay utilizing the RAW 264.7 murine macrophage cells in tissue culture to determine pro-inflammatory activity. Upon determination of activity, active fractions were analyzed utilizing liquid chromatography-mass spectrometry, MS/MS mapping, and high-performance liquid chromatography to isolate and determine the identities of any pro-inflammatory compounds. Subsequently, the isolated compounds were then tested again in the *in vitro* inflammatory response assay.

Chapter Two

Methods

2.1. Extraction of *L. polyedrum* cell culture

L. polyedrum cell cultures were provided by the Latz laboratory and grown in f/4 medium at 20°C on an alternating 12 hour light to 12 hour dark cycle. A total of 22.5 L of cell culture was then vacuum filtered through a Thermo Scientific Nalgene 150 mm porcelain Buchner funnel with Whatman 15 cm diameter 20-25 μ pore size qualitative filter paper to separate cells from cell media. The cells were left on the filter paper and extracted via submersion in 2:1 dichloromethane:methanol until solvent was colorless. This 2:1 DCM:MeOH extract was dried on a rotary evaporator to obtain the crude cell extract. The cell culture media was extracted utilizing Sigma-Aldrich Amberlite XAD16 resin. A total of 400 g of resin was conditioned by stirring resin for 10 minutes in the following solvent procedure: acetone, methanol, dichloromethane, a fresh volume of dichloromethane again, methanol, acetone, water, and water again, decanting the previous solvent between each solvent step. Once the resin was conditioned, 2.5 L aliquots of cell media were introduced to the resin and allowed to stir for an hour. The media was then decanted before introducing another 2.5 L of cell media to stir for another hour. This was repeated until all 22.5 L of cell culture was introduced to the resin. The resin was then extracted twice with two 300 mL volumes of 1:1 DCM/MeOH, followed by 300 mL of DCM, and then 300 mL of methanol. All 1200 mL of this media extraction was then combined and dried on a rotary evaporator to obtain the crude media extract.

2.2. Vacuum-liquid Chromatography Fractionation of *L. polyedrum* cell culture extraction

Dried crude *L. polyedrum* cell extract was fractionated using vacuum-liquid chromatography (VLC) into 9 fractions (Figure 2.1). The extract was fractionated over an Agilent 500 mg 3 mL cartridge of Normal Phase Silica SPE which was first conditioned with the first solvent, hexanes. The crude extract was then dissolved in a small volume of the first solvent and added to the column. Three column volumes of the first solvent were added to the column and the elution was collected. This process was repeated for all 9 solvent mixtures and all 9 fractions were dried down on a rotary evaporator.

Resin extracted cell culture media was fractionated into five fractions (Figure 2.2). The extract was fractionated over an Agilent 500 mg 3 mL cartridge of Reverse Phase Silica SPE which was first conditioned with the first solvent, 80% H₂O:20% Acetonitrile. The cell culture media extract was dissolved in a small volume of the first solvent and added to the column. Three column volumes of the first solvent were added to the column and the elution was collected. This process was repeated for all 5 solvent mixtures and all 5 fractions were dried down on a rotary evaporator.

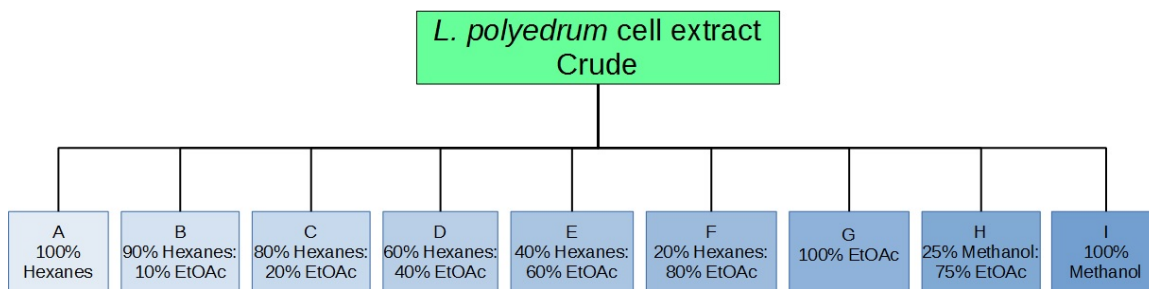


Figure 2.1. Vacuum-liquid Chromatography Fractionation of *L. polyedrum* cell extract. Crude extract of *L. polyedrum* cells was fractionated into the solvent mixtures presented above over 500 mg of Normal Phase silica gel.

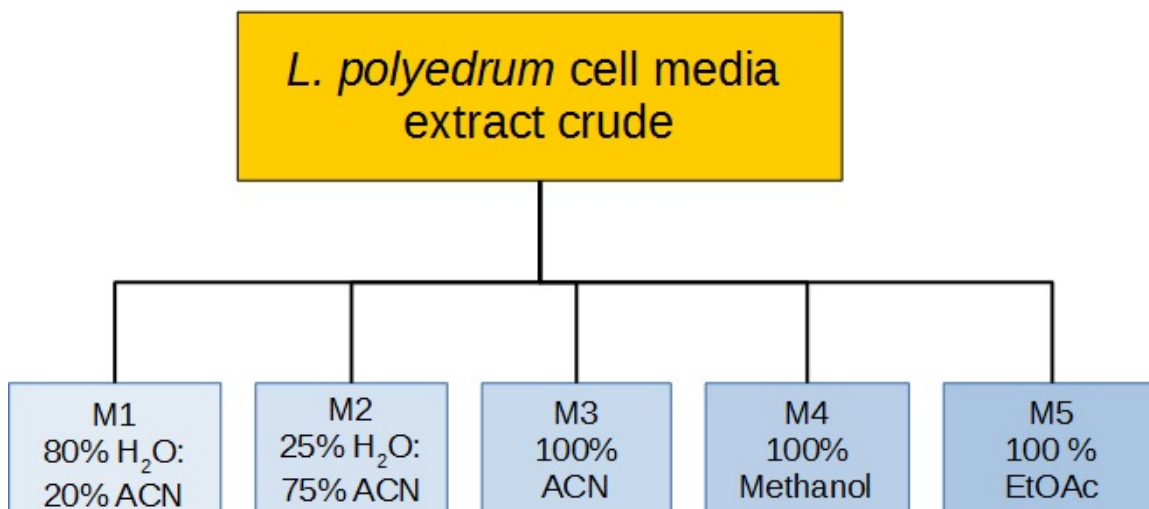


Figure 2.2. **Vacuum-liquid Chromatography Fractionation of *L. polyedrum* cell media extract.** Extract of *L. polyedrum* cell culture media was fractionated into the solvent mixtures presented above over 500 mg of Reverse Phase silica.

2.3. Extraction of *L. polyedrum* cell culture for yessotoxin-like metabolites

A total of 22.5 L of *L. polyedrum* cell culture was vacuum filtered through a Thermo Scientific Nalgene 150 mm porcelain Buchner funnel with Whatman 15 cm diameter 20-25 μ pore size qualitative filter paper to separate cells from cell media. The cells were left on the filter paper and extracted via submersion in 100% methanol until solvent was colorless. The solvent was evaporated off to obtain a dried extract which was subsequently dissolved and partitioned between 200 mL of hexanes and 200 mL of 4:1 methanol:H₂O in a 500 mL separatory funnel. The methanolic layer was separated and suspended in water and extracted with butanol. The three solvent layers, hexane, butanol, and aqueous, were dried down separately on a rotary evaporator.

2.4. Nitric oxide Inflammatory Response *in Vitro* assay

Inflammatory response was analyzed by measuring nitric oxide formation in RAW 264.7 murine macrophage tissue cultures. RAW 264.7 cells were seeded onto 96-well plates with 5×10^4 cells per well and allowed to incubate for 24 hours in Sigma-Aldrich Dulbecco's Modified Eagle's Medium (DMEM) in 10% endotoxin free fetal bovine serum (FBS) at 37°C and 5.0% CO₂. After 24 hours, controls and fractions dissolved in 100% ethanol for testing were added to plates in triplicate, allowed to incubate for an hour, and then 10 µL of 60 ug/mL lipopolysaccharide in water was added to controls while all other wells, including wells containing cell extract fractions, received 10 uL of phosphate buffer solution (PBS). Lipopolysaccharide was used as a positive control to induce an inflammatory response at a final concentration of 3 ug/mL, a final concentration of 1.5% ethanol was used as a reference control, and a final well concentration of 1.0% DMSO with 3 ug/mL of LPS was used as another control as DMSO is an inhibitor of inflammatory response. *L. polyedrum* fractions were dissolved in ethanol and tested at the following final concentrations in the well : 30 ug/mL, 10 ug/mL, 3 ug/mL, 1 ug/mL, 0.3 ug/mL, and 0.1 ug/mL. The cells were incubated for 24 hours and 50 uL of media from each testing well was transferred to a new 96-well plate in duplicate. A nitrite standard curve was prepared by diluting nitrite stock solution to the following concentrations in DMEM in 10% FBS to a total volume of 50 uL: 100 uM, 50 uM, 25 uM, 12.5 uM, 6.25 uM, 3.13 uM, 1.56 uM, and 0 uM. Sulfanilamide solution (1% sulfanilamide in 5% phosphoric acid) was added in 50 uL aliquots to each well and allowed to incubate at room temperature for 10 minutes in the dark to allow NO₂⁻, a stable product of nitric oxide, to react and form diazonium salt. After 10 minutes, 50 uL

of NED solution (0.1% N-1-naphthylethylenediamine dihydrochloride in water) was added to each well and the plates were allowed to incubate for another 10 minutes in the dark. The absorbance of the solutions were then read on a plate reader at a wavelength of 570 nm.

2.5. Cell proliferation *in Vitro* assay

After the media was removed from the wells for nitric oxide assay, the remaining cell media was aspirated off leaving only the RAW264.7 cells at the bottom of the 96 well plates. 3-(4,5-dimethylthiazol-2-yl)-2,5-diphenyltetrazolium bromide (MTT) at 5 mg/mL was added to DMEM without FBS in 1:5 ratio of MTT to DMEM and 60 uL of this mixture was added to each well the aspirated RAW264.7 cell plate. The plate is then placed back in the 37°C/5.0% CO₂ incubator for 25 minutes to allow the remaining living cells to reduce the MTT to formazan. After this incubation, the MTT solution was aspirated off and the plate was placed back into the incubator with the lid off for 20 minutes to allow the rest of the solution to evaporate. The next step was to add 100 uL of DMSO into a each well to solubilize the formazan product. The plates were then read on a plate reader at 570 nm and 630 nm.

2.6. Liquid chromatography-mass spectrometry analysis

The *L. polyedrum* cell and cell culture media fractions as well as HPLC fractions were analyzed using a Thermo Finnigan LCQ AdvantageMax mass detector with an electrospray ionization source in positive mode, Thermo Finnigan Surveyor Autosampler-Plus, a LC-Pump-Plus, and PDA-Plus system. The ESI conditions were as follows: 325°C capillary temperature, 5 kV source voltage, and 69 psi sheath gas flow rate. Acetonitrile (solvent A) and H₂O with 0.1% formic acid (solvent B) were the two

solvents used at a flow rate of 0.7 mL/min. Initially the flow was a constant flow of 5% solvent A and 95% solvent B for 5 minutes which was followed by a linear gradient to 95% solvent A and 5% solvent B over 10 minutes and then held for 5 minutes. This hold was followed by a linear gradient back to initial solvent conditions of 5% solvent A and 95% solvent B over 1 minute which is held for another 4 minutes. A Phenomenex Kinetex 5 μm C₁₈ column (150 x 4.6 mm) was used for the two scan events, first a mass search range of m/z 150-2000 followed by MS² scans dependent on the data from the first scan event. High-resolution electrospray ionization mass spectrometry (HRESIMS) was also utilized to analyze the HPLC fractions. An Agilent 1290 Infinity system with Agilent 6530 Accurate Mass Q-TOF LC/MS was utilized with a Phenomenex Kinetex 5 μm C₁₈ 150 x 4.6 mm column and the same solvent gradient was utilized for both machines.

2.7. MS/MS Molecular Networking

Utilizing MS/MS fragmentation patterns from LCMS analysis of *L. polyedrum* fractions, a molecular network was generated which correlated similar molecules based on their MS²-fragmentation patterns (<http://gnps.ucsd.edu/ProteoSAFe/static/gnps-splash.jsp>). This network was visualized in Cytoscape wherein circular nodes denoted parent masses and cosine similarities between parent masses were denoted by edges (lines) linking nodes. The thicker a node, the higher the cosine value indicating higher similarity.

2.8. Isolation of Digalactosyldiacylglycerol (20:5/18:5) and Monogalactosyldiacylglycerol (20:5/18:5)

Isolation of digalactosyldiacylglycerol (20:5/18:5) (DGDG(20:5/18:5)) and monogalactosyldiacylglycerol (20:5/18:5) (MGDG(20:5/18:5)) began with high-

performance liquid chromatography to isolate the desired DGDG from fraction E of the *L. polyedrum* cell extract and MGDG from fraction F also of the cell extract. A Waters 515 pump system linked to a Waters 996 PDA was utilized to perform this HPLC. Samples were dissolved in 1:1 H₂O:MeOH and run isocratically using 85% H₂O/15% MeOH with a Synergi 4 μm Hydro-RP 250 x 10.00 mm column.

2.9. 1D NMR Analysis of *L. polyedrum* Fractions

1D NMR analysis of fraction F of *L. polyedrum* cell extract was performed utilizing a Varian Unity 500 MHz spectrometer. The fraction was dissolved in deuterated chloroform (CDCl₃) and filtered to remove any particulates in the sample. A total of 64 scans were performed.

Chapter Three

Assay-guided Extraction of *L. polyedrum* Cell Culture

3.1. *L. polyedrum* Cell Culture Extraction

L. polyedrum cell cultures, a total of 22.5 L provided by the Latz laboratory at the Scripps Institution of Oceanography, first required extraction by separating the cells from cell media. Cultured *L. polyedrum* was utilized as it is more readily available due to the sporadic nature of the *L. polyedrum* blooms. Vacuum filtration of the cultures was done utilizing a Buchner funnel and Whatman filter paper with a 20-25 μm pore size. This pore size is small enough to prevent an average *L. polyedrum* cell, roughly 40-54 μm in length and 37-53 μm in width, from filtering through the funnel while storing the flow-through cell media for later extraction. However, as the cell cultures were not dense and, due to the difficulty of separating the cells from the filter paper, it was decided no dry cellular biomass was to be obtained and instead the primary extraction of the cells in 2:1 dichloromethane:methanol was to be done by soaking the cells with the filter paper. After this initial extraction of cells, the extract was dried to afford a total of 44 mg of crude *L. polyedrum* extract, 4 mg of which was stored to test as a crude while the remaining 40 mg was utilized in the VLC fractionation, the results of which are shown in Figure 3.1.

The cell media was stored after filtration of *L. polyedrum* cells and also extracted through the use of Amberlite XAD16 resin. After conditioning of resin, 2.5 L of cell filtrate was introduced to the resin and stirred for an hour and allowed to settle before decanting and addition of fresh cell filtrate. This process was repeated until all 22.5 L of filtrate was introduced to the resin. The charged resin was then extracted twice with 300 mL volumes of 1:1 dichloromethane:methanol, then 300 mL of dichloromethane, and finally with 300 mL of methanol. These extracts were all combined and dried down to afford 6.0137 g of extract, though it appeared a large amount of the sample was

composed of salt. All of the extract was subject to VLC fractionation to give 5 fractions as shown in Figure 3.2.

It is pertinent to note that during the process of working with the cell cultures, two researchers experienced some minor respiratory difficulties and lightheadedness. This necessitated the use of face masks for all subsequent work done with the cell culture.

3.2. Nitric Oxide Inflammatory Response and Cell Proliferation Assay of *L.*

***polyedrum* Extraction**

After the initial extraction of the *L. polyedrum* cultures, the fractions were tested using the RAW264.7 murine macrophage cultures to determine if a potential inflammatory response, as measured by an increase in the nitric oxide production, was induced by the fractions. The MTT cell staining assay was also utilized to determine whether the fractions had any effect on cell viability.

Upon observation of the results, the highest concentration of fractions used, 30 $\mu\text{g/mL}$, shown in Figure 3. 3, had a large cytotoxic effect on the cells with most of the fractions resulting in below 50% cell survival and minimal inflammatory response. At 10 $\mu\text{g/mL}$, shown in Figure 3.4, there was still some cytotoxicity in fractions B-G, however there was now some significant inflammatory response in the Crude, A, C, D, F, and G. Fraction G interestingly had over 200% inflammatory response but was also significantly cytotoxic at 25%. Dropping to 3 $\mu\text{g/mL}$, shown in Figure 3.5, fractions A, B, F, and I showed an inflammatory response, with fraction F having much the same response as it did at 10 $\mu\text{g/mL}$. There was still significant cytotoxicity in fractions E, F, and G. At 1 $\mu\text{g/mL}$ and lower concentrations (Figures 3.6, 3.7, and 3.8), the fractions no longer elicited a cytotoxic effect, however most of the inflammatory response was also absent.

The cell media extract fractions were also tested at the same concentrations, however the results at all concentrations did not display significant inflammatory response or cytotoxicity.

From these results, it was decided that fractions F and G were to be further investigated to determine the presence of any pro-inflammatory compounds as these fractions induced the highest nitric oxide production.

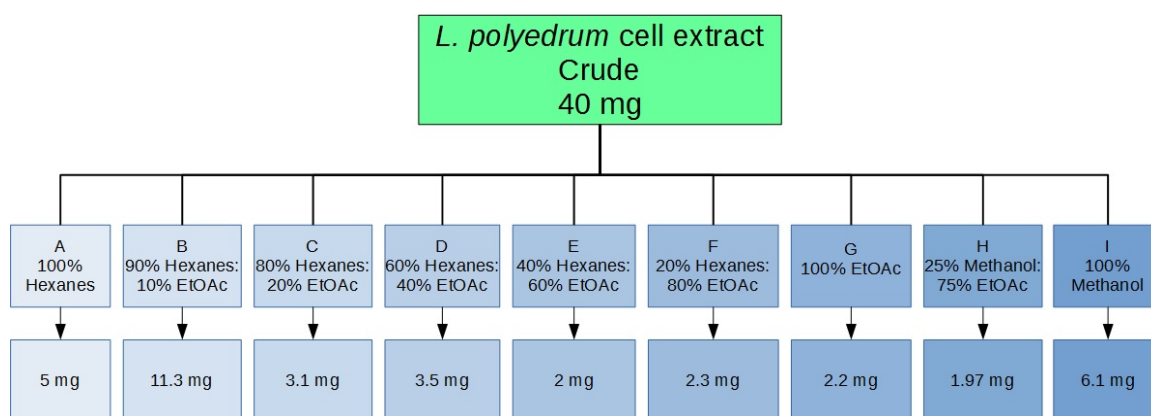


Figure 3.1. **Vacuum-liquid Chromatography Fractionation of *L. polyedrum* cell extract.** Dried crude extract of *L. polyedrum* cells was fractionated into the solvent mixtures presented above over 500 mg of Normal Phase silica. A 40. mg sample of crude extract was fractionated into the 9 fractions as shown above after rotary evaporation and overnight lyophilization.

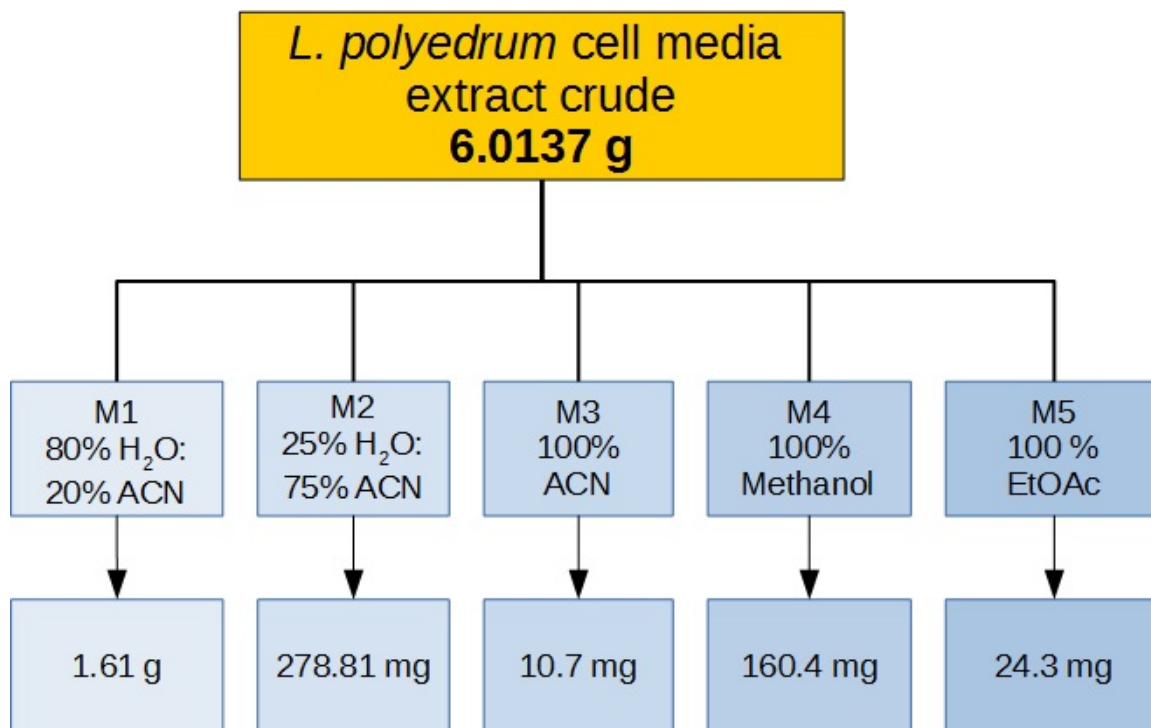


Figure 3.2. **Vacuum-liquid Chromatography Fractionation of *L. polyedrum* cell media extract.** Dried crude cell media extract of *L. polyedrum* cells extracted via Amberlite XAD16 resin was fractionated into the solvent mixtures presented above over 500 mg of Normal Phase silica. A total of 6.0137 grams of crude extract were fractionated into the 5 fractions as shown above after rotary evaporation and overnight lyophilization.

Nitric Oxide Production and Cytotoxicity of *L. polyedrum* Cell Extract
30 $\mu\text{g/mL}$

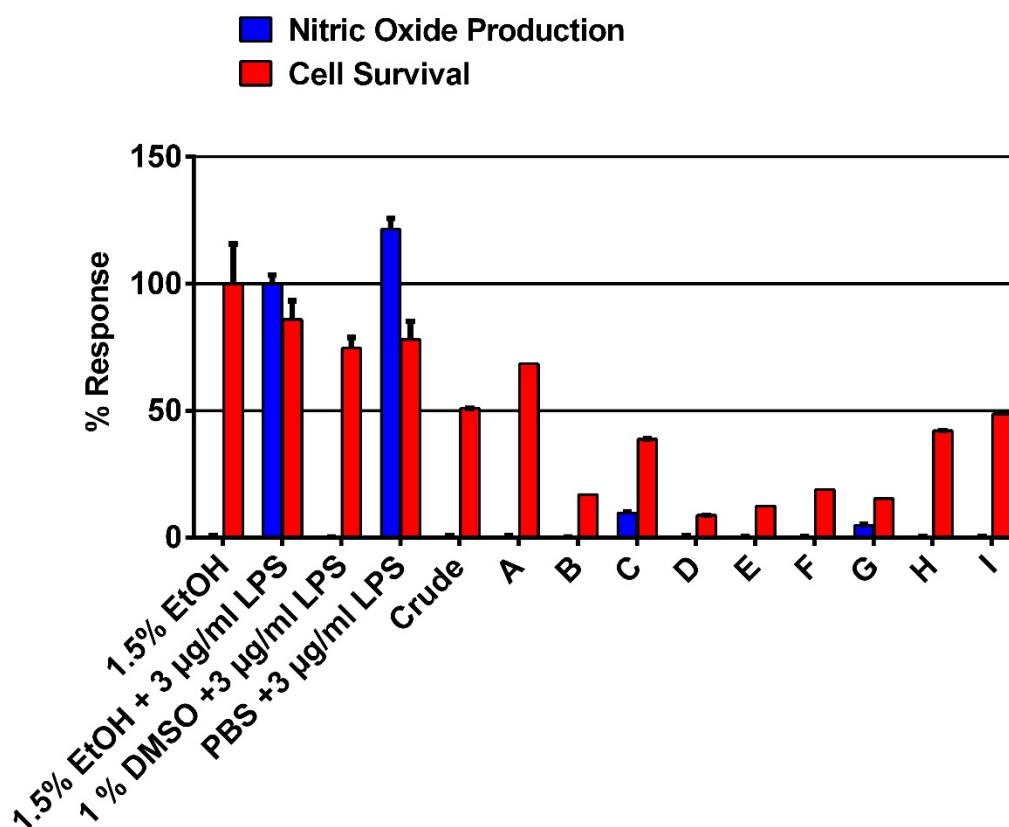


Figure 3.3. *L. polyedrum* cell fraction Inflammation and Cytotoxicity Assay at 30 $\mu\text{g/mL}$. *L. polyedrum* cell extract fractions were introduced to RAW264.7 murine macrophage cells. Fractions were dissolved in ethanol and introduced to the cells at a final concentration of 30 $\mu\text{g/mL}$ in triplicate and allowed to incubate for 24 hours before testing the cell media solution for nitric oxide concentration utilizing the Griess reagent reaction. The remaining RAW264.7 cells were then aspirated and tested in a cell proliferation assay utilizing MTT staining. The first four columns represent the four controls: 1.5% ethanol, 1.5% ethanol with 3 $\mu\text{g/mL}$ LPS, 1.0% DMSO with 3 $\mu\text{g/mL}$ LPS, and 1.5% PBS with 3 $\mu\text{g/mL}$. The data shown utilizes the response of the positive control, 3 $\mu\text{g/mL}$ LPS in 1.5% ethanol, as the base 100% response for nitric oxide production and cell survival.

Nitric Oxide Production and Cytotoxicity of *L. polyedrum* Cell Extract 10 $\mu\text{g}/\text{mL}$

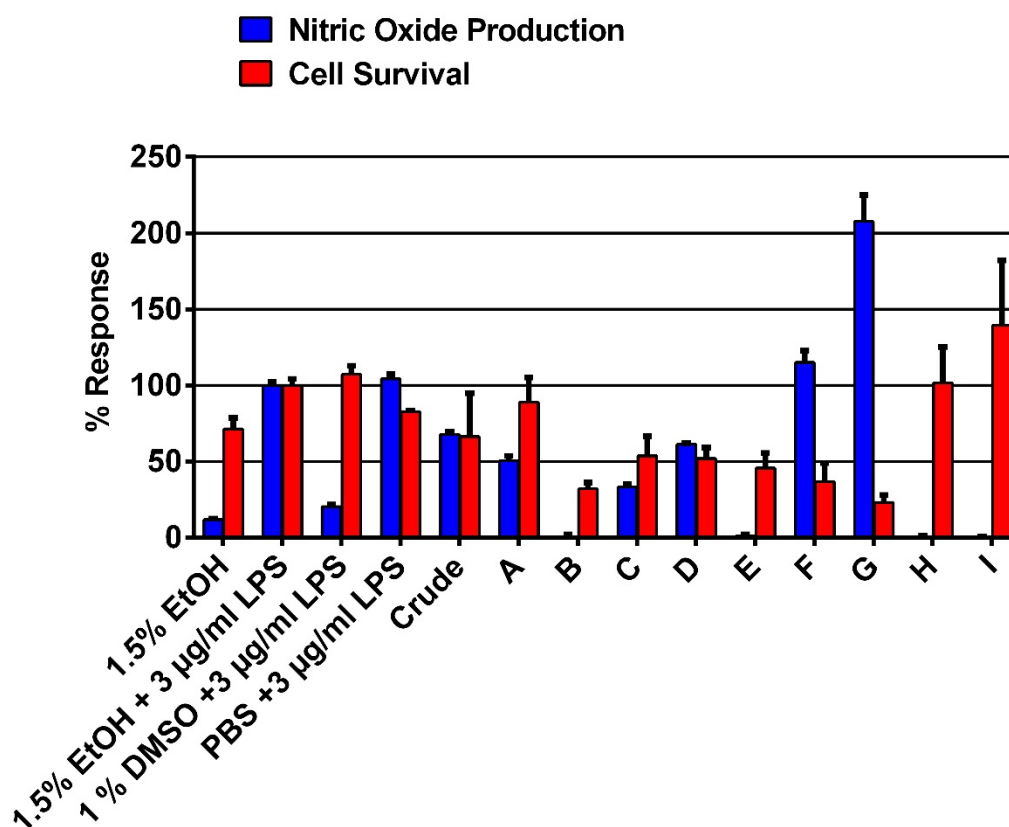


Figure 3.4. *L. polyedrum* cell fractions tested. **Increase in NO production and Cytotoxicity at 10 $\mu\text{g}/\text{mL}$.** *L. polyedrum* cell extract fractions were introduced to RAW264.7 murine macrophage cells. Fractions were dissolved in ethanol and introduced to the cells at a final concentration of 10 $\mu\text{g}/\text{mL}$ in triplicate and allowed to incubate for 24 hours before testing the cell media solution for nitric oxide concentration utilizing the Griess reagent reaction. The remaining RAW264.7 cells were then aspirated and tested in a cell proliferation assay utilizing MTT staining. The first four columns represent the four controls: 1.5% ethanol, 1.5% ethanol with 3 $\mu\text{g}/\text{mL}$ LPS, 1.0% DMSO with 3 $\mu\text{g}/\text{mL}$ LPS, and 1.5% PBS with 3 $\mu\text{g}/\text{mL}$. The data shown utilizes the response of the positive control, 3 $\mu\text{g}/\text{mL}$ LPS in 1.5% ethanol, as the base 100% response for nitric oxide production and cell survival.

Nitric Oxide Production and Cytotoxicity of *L. polyedrum* Cell Extract
3 $\mu\text{g}/\text{mL}$

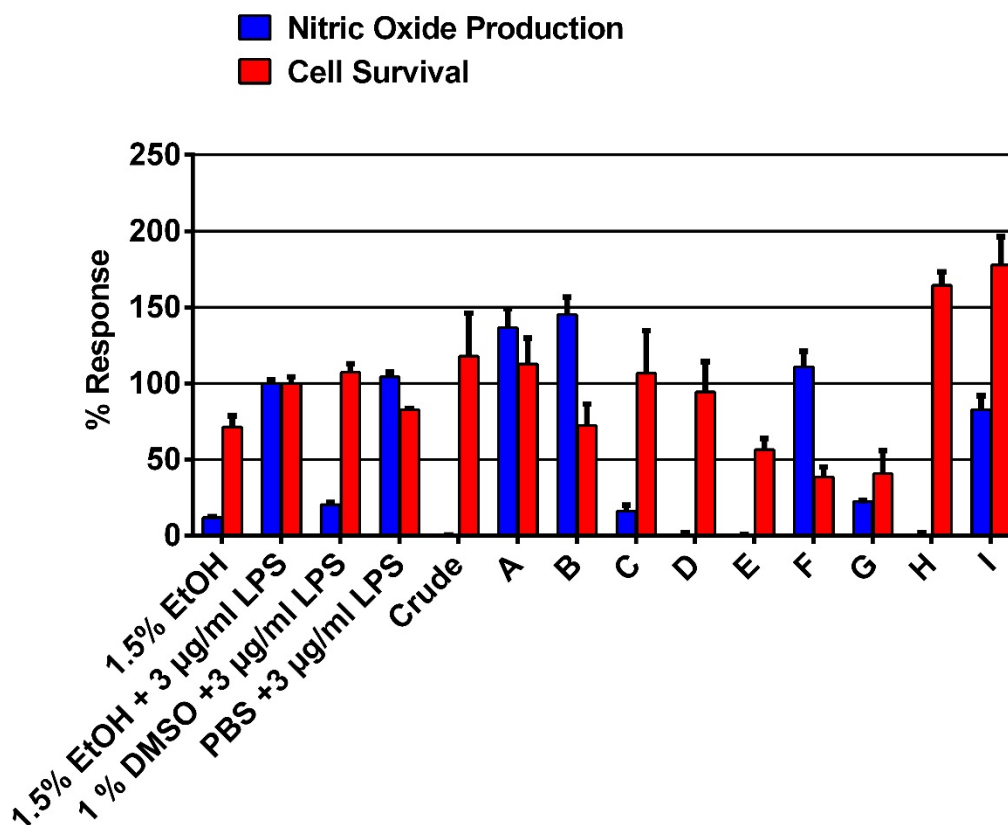


Figure 3.5. *L. polyedrum* cell fraction Inflammation and Cytotoxicity Assay at 3 $\mu\text{g}/\text{mL}$. *L. polyedrum* cell extract fractions were introduced to RAW264.7 murine macrophage cells. Fractions were dissolved in ethanol and introduced to the cells at a final concentration of 3 $\mu\text{g}/\text{mL}$ in triplicate and allowed to incubate for 24 hours before testing the cell media solution for nitric oxide concentration utilizing the Griess reagent reaction. The remaining RAW264.7 cells were then aspirated and tested in a cell proliferation assay utilizing MTT staining. The first four columns represent the four controls: 1.5% ethanol, 1.5% ethanol with 3 $\mu\text{g}/\text{mL}$ LPS, 1.0% DMSO with 3 $\mu\text{g}/\text{mL}$ LPS, and 1.5% PBS with 3 $\mu\text{g}/\text{mL}$. The data shown utilizes the response of the positive control, 3 $\mu\text{g}/\text{mL}$ LPS in 1.5% ethanol, as the base 100% response for nitric oxide production and cell survival.

Nitric Oxide Production and Cytotoxicity of *L. polyedrum* Cell Extract
1 $\mu\text{g}/\text{mL}$

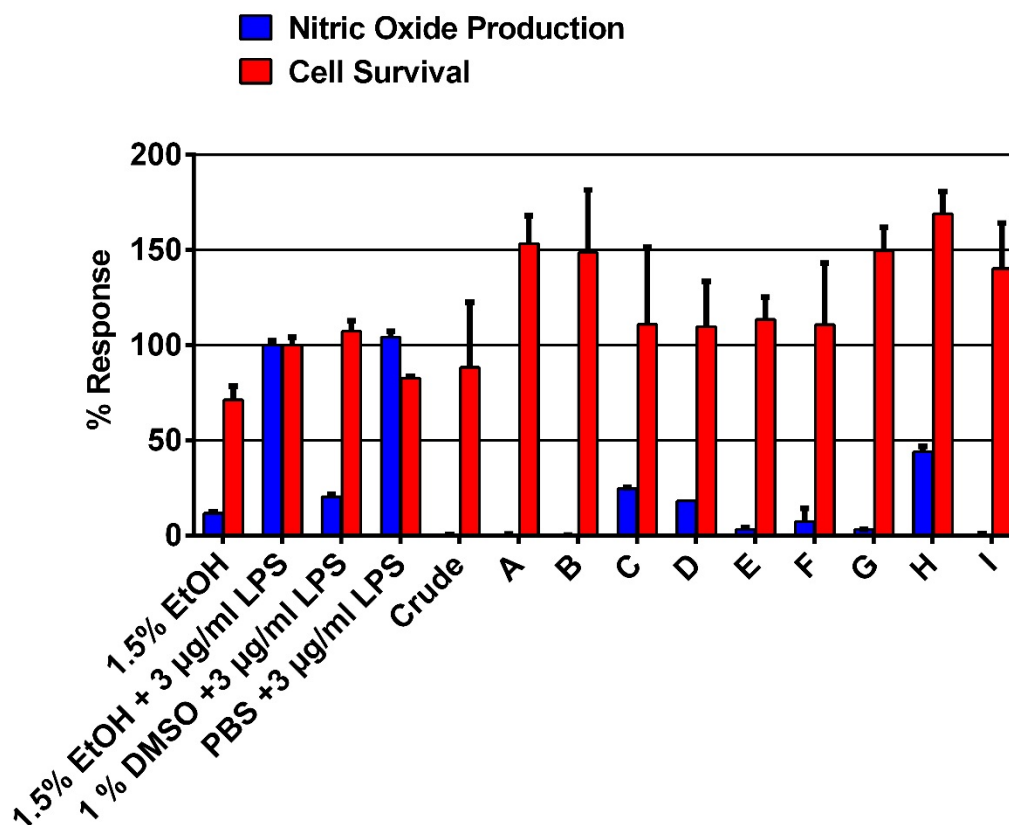


Figure 3.6. *L. polyedrum* cell fraction Inflammation and Cytotoxicity Assay at 1 $\mu\text{g}/\text{mL}$. *L. polyedrum* cell extract fractions were introduced to RAW264.7 murine macrophage cells. Fractions were dissolved in ethanol and introduced to the cells at a final concentration of 1 $\mu\text{g}/\text{mL}$ in triplicate and allowed to incubate for 24 hours before testing the cell media solution for nitric oxide concentration utilizing the Griess reagent reaction. The remaining RAW264.7 cells were then aspirated and tested in a cell proliferation assay utilizing MTT staining. The first four columns represent the four controls: 1.5% ethanol, 1.5% ethanol with 3 $\mu\text{g}/\text{mL}$ LPS, 1.0% DMSO with 3 $\mu\text{g}/\text{mL}$ LPS, and 1.5% PBS with 3 $\mu\text{g}/\text{mL}$. The data shown utilizes the response of the positive control, 3 $\mu\text{g}/\text{mL}$ LPS in 1.5% ethanol, as the base 100% response for nitric oxide production and cell survival.

Nitric Oxide Production and Cytotoxicity of *L. polyedrum* Cell Extract 0.3 $\mu\text{g}/\text{mL}$

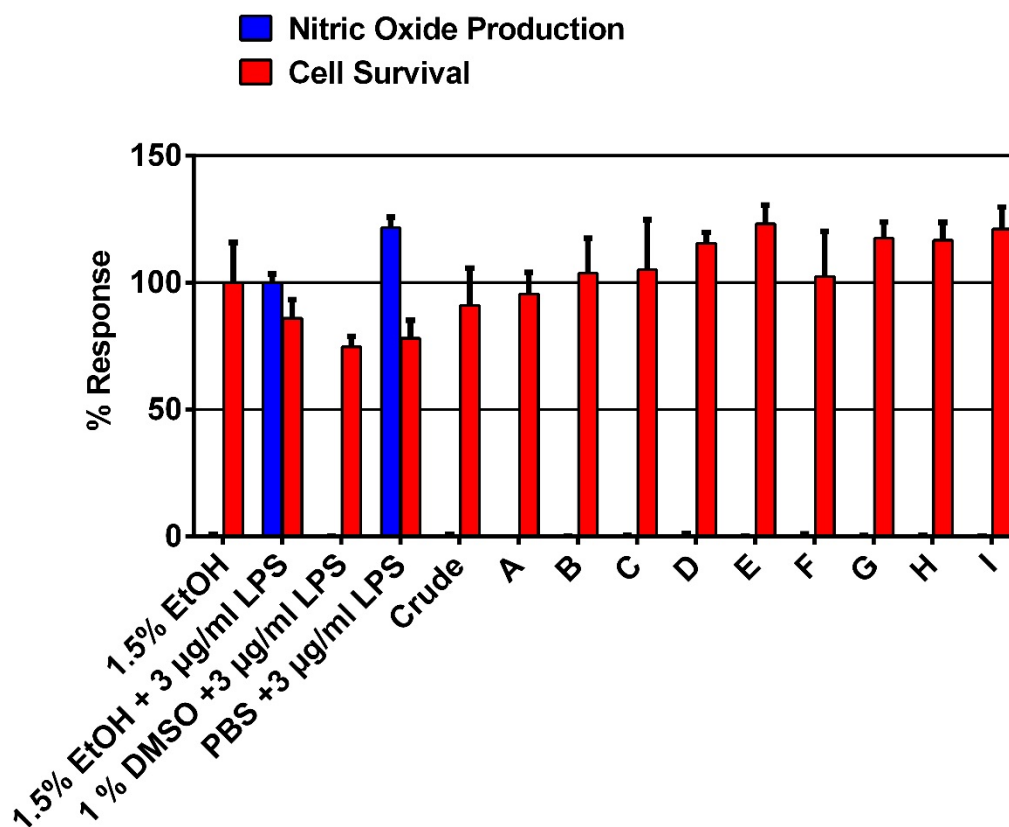


Figure 3.7. *L. polyedrum* cell fraction Inflammation and Cytotoxicity Assay at 0.3 $\mu\text{g}/\text{mL}$. *L. polyedrum* cell extract fractions were introduced to RAW264.7 murine macrophage cells. Fractions were dissolved in ethanol and introduced to the cells at a final concentration of 0.3 $\mu\text{g}/\text{mL}$ in triplicate and allowed to incubate for 24 hours before testing the cell media solution for nitric oxide concentration utilizing the Griess reagent reaction. The remaining RAW264.7 cells were then aspirated and tested in a cell proliferation assay utilizing MTT staining. The first four columns represent the four controls: 1.5% ethanol, 1.5% ethanol with 3 $\mu\text{g}/\text{mL}$ LPS, 1.0% DMSO with 3 $\mu\text{g}/\text{mL}$ LPS, and 1.5% PBS with 3 $\mu\text{g}/\text{mL}$. The data shown utilizes the response of the positive control, 3 $\mu\text{g}/\text{mL}$ LPS in 1.5% ethanol, as the base 100% response for nitric oxide production and cell survival.

Nitric Oxide Production and Cytotoxicity of *L. polyedrum* Cell Extract
0.1 $\mu\text{g}/\text{mL}$

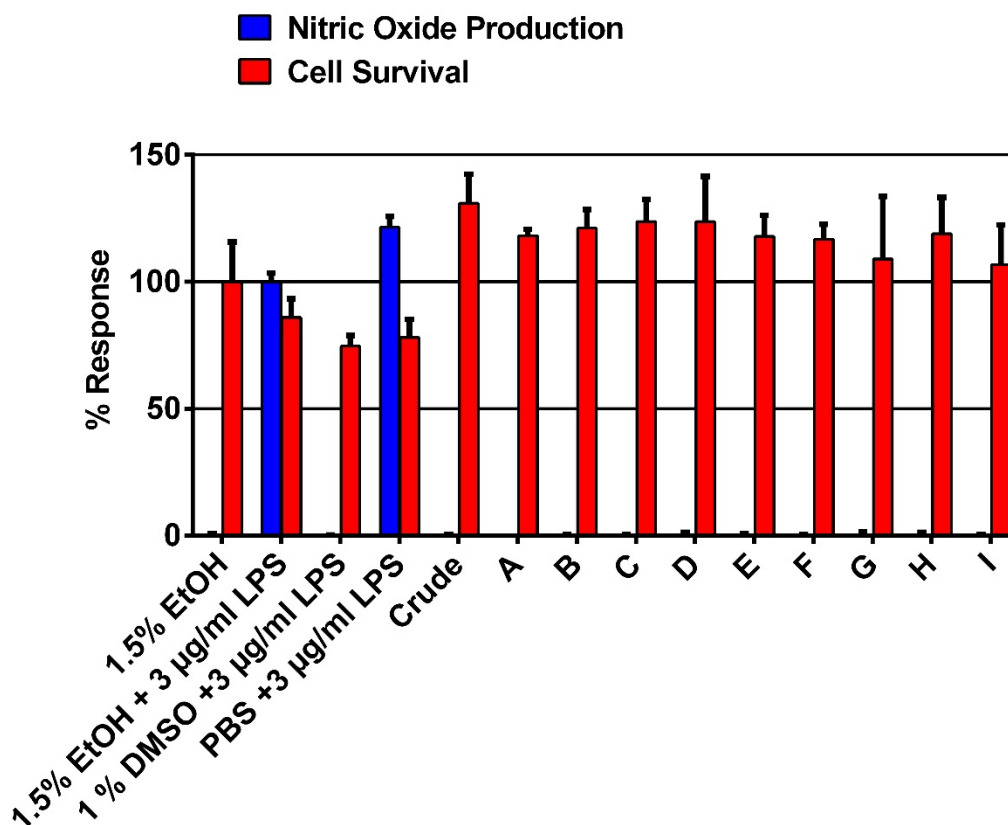


Figure 3.8. *L. polyedrum* cell fraction Inflammation and Cytotoxicity Assay at 0.1 $\mu\text{g}/\text{mL}$. *L. polyedrum* cell extract fractions were introduced to RAW264.7 murine macrophage cells. Fractions were dissolved in ethanol and introduced to the cells at a final concentration of 0.1 $\mu\text{g}/\text{mL}$ in triplicate and allowed to incubate for 24 hours before testing the cell media solution for nitric oxide concentration utilizing the Griess reagent reaction. The remaining RAW264.7 cells were then aspirated and tested in a cell proliferation assay utilizing MTT staining. The first four columns represent the four controls: 1.5% ethanol, 1.5% ethanol with 3 $\mu\text{g}/\text{mL}$ LPS, 1.0% DMSO with 3 $\mu\text{g}/\text{mL}$ LPS, and 1.5% PBS with 3 $\mu\text{g}/\text{mL}$. The data shown utilizes the response of the positive control, 3 $\mu\text{g}/\text{mL}$ LPS in 1.5% ethanol, as the base 100% response for nitric oxide production and cell survival.

Chapter Four

Identification and Isolation of Digalactosyldiacylglycerol (20:5/18:5) and

Monogalactosyldiacylglycerol (20:5/18:5)

4.1 Liquid Chromatography-Mass Spectrometry Analysis of Active *L. polyedrum*

Fractions

Upon deciding which active fractions to investigate, the fractions were analyzed by liquid chromatography-mass spectrometry. Fractions tested were dissolved in methanol to 1 mg/mL. The solvents used were acetonitrile, solvent A, and water with 0.1% formic acid, solvent B. Initially the flow was at a constant concentration of 5% solvent A and 95% solvent B for 5 minutes which was followed by a linear gradient to 95% solvent A and 5% solvent B over 10 minutes which was held for 5 minutes. This hold was followed by a linear gradient back to initial solvent conditions of 5% solvent A and 95% solvent B over 1 minute which is held for another 4 minutes.

Upon analysis of fractions F and G, Figures 4.2 and 4.3 respectively, both shared a chromatographic peak at 18.50 minutes and in each case gave an MS¹ spectrum with an 817 *m/z* ion. The MS² spectra of these 817 *m/z* ions showed the same fragment ions at 515 *m/z* and 543 *m/z* ions, indicating that these peaks are most likely the same molecule in both fractions. Upon comparison of the chromatograms of the two fractions, fraction G has a higher abundance of the 18.50 minute peak ion.

4.2. Molecular Networking of *L. polyedrum* Extraction

The *L. polyedrum* cell extracts, as well as cell media extracts, were run on LCMS and the generated MS¹ and MS² data were combined to generate a molecular network, shown in Figure 4.4, utilizing the molecular network platform provided by Global Natural Products Social Molecular Networking (GNPS). A network was generated in order to determine if there were known pure compounds similar to the ion of interest or whether there were similar molecules within the other cell extracts. The network

generated was also run with GNPS along with the pure compound libraries from the Gerwick laboratory to search for any known matching ions. The orange nodes in Figure 4.4 represent ions from the Gerwick lab pure compound library. As indicated, none of the major ions from the *L. polyedrum* fractions were found to be similar to any known pure compounds available in the library.

The network was then pared down to show only the *L. polyedrum* fractions, as shown in Figure 4.5. In this figure, red nodes represent molecules from Fraction F and G, yellow fractions represent molecules from Fraction E, green nodes represent molecules from media fraction M4, and blue nodes represent molecules from media fraction M5. The peak of interest from fractions F and G was shown to have a high similarity to a 979 m/z ion from fraction E with a cosine value of 0.933. These data suggested that fraction E had an ion very similar to the 817 m/z ion of interest. As seen in the LCMS results of fraction E, Figure 4.1, there was indeed a 979 m/z ion at 16.68 minutes.

4.3. 1D Proton NMR Analysis of Active *L. polyedrum* Fractions

The next step in determining the identity of the compound of interest was to perform a 1D proton NMR analysis of Fraction F. A sample of fraction F was dissolved in deuterated chloroform and filtered to remove particulates which then was analyzed on a Varian Unity 500 MHz spectrometer, the results of which are shown in Figure 4.6. Analysis of the spectrum reveals some features of the structure of this compound. The large peak at 5.4 ppm seems to indicate high number of alkene groups, while a peak at 2.35 ppm indicates protons alpha to a carbonyl group. The high number of peaks from 4.1 ppm to 3.5 ppm may also suggest a sugar group. These results point toward the possible structure of the molecule being a glycolipid with unsaturated lipid chains.

4.4. Determination of Monogalactosyldiacylglycerol (20:5/18:5) as the Molecule of Interest

With the results of the NMR analysis suggesting that the 817 m/z compound may be a glycolipid, research was done to determine whether *L. polyedrum* was a known producer of any glycolipids matching this description. It was found that *L. polyedrum* is a known producer of the glycolipids monogalactosyldiacylglycerol (MGDG) and digalactosyldiacylglycerol (DGDG) with one of the major forms of MGDG being MGDG (20:5/18:5), structure shown in Figure 4.10, which has a molecular weight of 817 which matches our molecule of interest (Gray, CG et al 2009). These glycolipids are key components of the chloroplast membranes for *L. polyedrum* and other dinoflagellates. DGDG was shown to follow a common MS² fragmentation pattern, specifically, first the loss of a galactose unit to form MGDG and then the loss of either of the fatty acid chains. With this in mind, the high similarity between the 979 m/z ion from fraction E and the 817 m/z ion from Fraction F and G, seen in Figure 4.5, aligns well with the 979 m/z ion being DGDG (20:5/18:5), structure shown in Figure 4.9, as the difference between the two masses is 162 daltons, the mass of one galactose group. Furthermore, analysis of the MS² spectrum of fraction E, shown in Figure 4.1, displays two other ions, 677 m/z and 705 m/z . The difference between the parent ion 979 m/z and 677 m/z is 302 daltons which is the molecular weight of a 20:5 unsaturated fatty acid chain, while the difference between 979 m/z and 705 m/z is 274 daltons, which is the molecular weight of an 18:5 unsaturated fatty acid chain. These data strongly implicate that these two peaks represent the loss of those specific unsaturated fatty acid chains. Analysis of the 817 m/z MS² spectra from either fraction F or G also displayed two ions at 515 m/z and 543 m/z , which

are also the same differences in mass. These data highly suggest that the molecule of interest is indeed MGDG (20:5/18:5).

To further identify the molecule found in Fraction F and G, a predicted 1D proton NMR was generated from the structure of MGDG (20:5/18:5) in ChemDraw, shown in Figure 4.7. Comparing the two spectra, they both share a majority of peaks, again suggesting that this structure is the molecule of interest.

4.5. High-performance Liquid Chromatography Isolation of Digalactosyldiacylglycerol (20:5/18:5) and Monogalactosyldiacylglycerol (20:5/18:5)

With the molecule of interest identified, the next step was to isolate these molecules in larger amounts from the fraction samples for further biological testing. High-performance liquid chromatography (HPLC) was utilized to isolate MGDG (20:5/18:5) from fractions F and G and DGDG (20:5/18:5) from fraction E. Samples were dissolved in 1:1 H₂O:methanol before being run on an isocratic gradient of 85% H₂O and 15% methanol on a Synergi 4 μm Hydro-RP 250 x 10.00 mm column. A total of 1.2 mg of MGDG (20:5/18:5) and 0.8 mg of DGDG (20:5/18:5) was isolated and confirmed by LCMS analysis.

4.6. Nitric Oxide Inflammatory Response and Cell Proliferation Assay of Digalactosyldiacylglycerol (20:5/18:5) and Monogalactosyldiacylglycerol (20:5/18:5)

After isolation of both glycolipids, the molecules were then tested in the nitric oxide inflammatory response and cell proliferation assays. Both glycolipids were prepared and the assays were tested utilizing the same protocol and conditions that had been used to test the crude *L. polyedrum* fractions. Figure 4.11 displays the results for the testing of DGDG (20:5/18:5) and Figure 4.12 displays the results for MGDG (20:5/18:5).

Surprisingly, neither of these glycolipids elicited significant inflammatory response in the RAW264.7 cells and also did not display any cytotoxicity. There is some apparent inflammatory response in the DGDG (20:5/18:5) results, however, it is the same amount of NO production as the vehicle control (1.5% ethanol), so it is unlikely that these are positive results. Thus, although the glycolipid MGDG (20:5/18:5) was the major component of the most active *L. polyedrum* fraction F, it does not elicit an inflammatory response on its own.

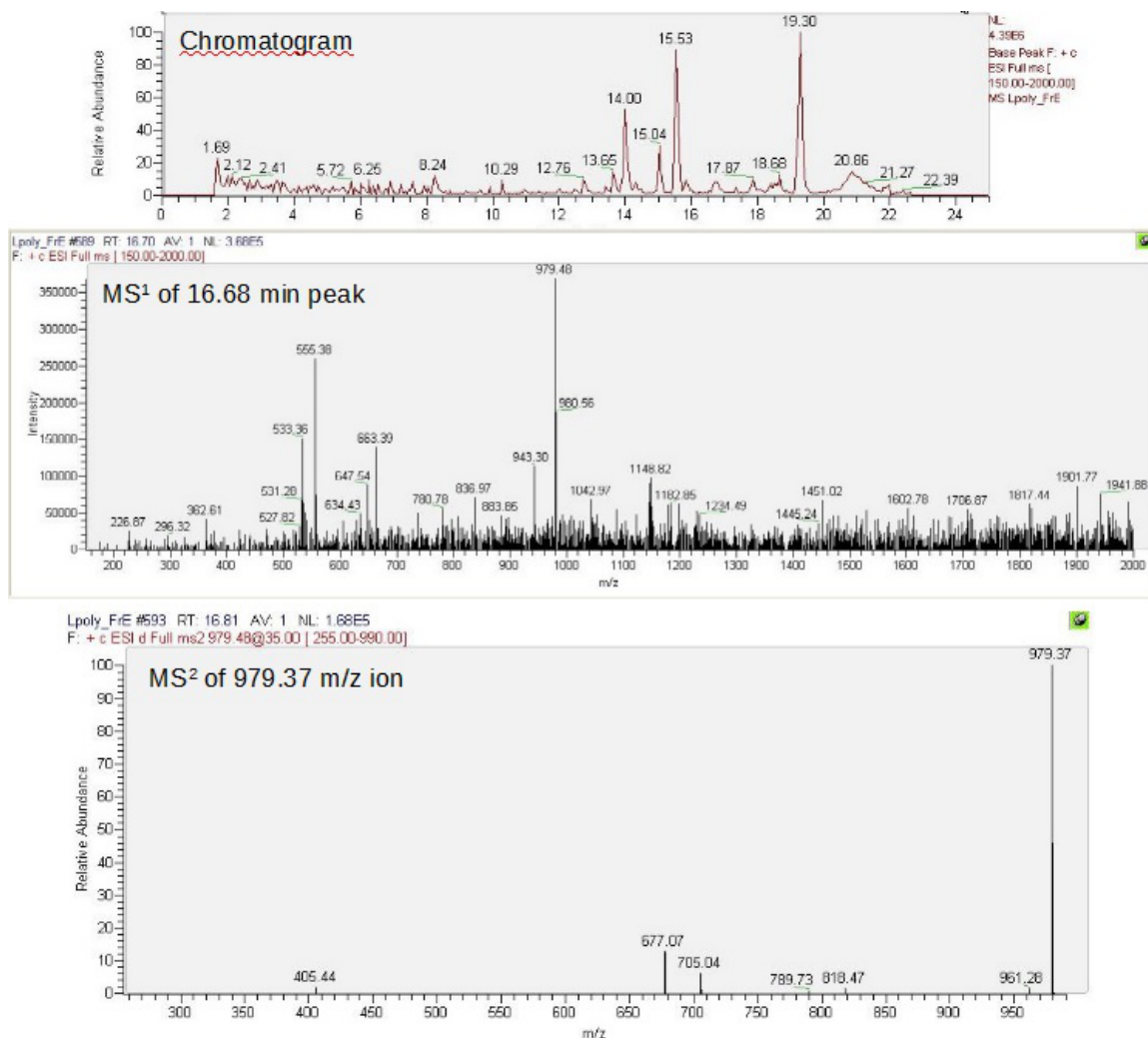


Figure 4.1. Liquid Chromatography-Mass Spectrometry Analysis of Fraction E. Liquid chromatography-mass spectrometry analysis was performed on Fraction E of the *L. polyedrum* cell extract. The analysis was performed on a Phenomenex Kinetex 5 μ m C₁₈ column (150 x 4.6 mm) using acetonitrile and H₂O with 0.1% formic acid as the two solvents in a linear gradient over 25 minutes at a flow rate of 0.7 mL/min. The top graph is the chromatogram of the sample while the middle is the MS¹ spectrum of the chromatogram peak at 16.68 minutes. The bottom spectrum is the MS² spectrum of the 979 m/z ion.

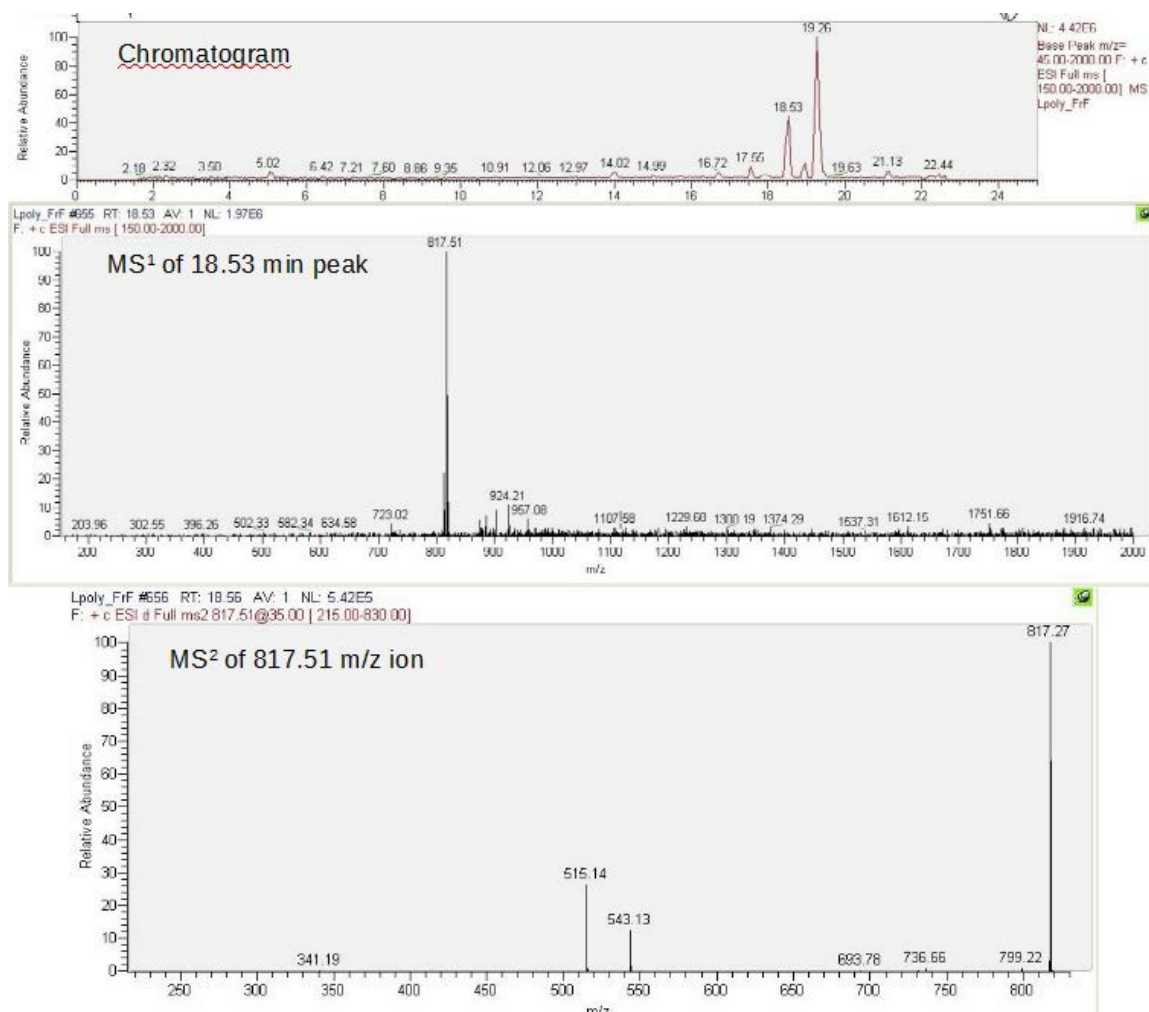


Figure 4.2. Liquid Chromatography-Mass Spectrometry Analysis of Fraction F. Liquid chromatography-mass spectrometry analysis was performed on Fraction F of the *L. polyedrum* cell extract. The analysis was performed on a Phenomenex Kinetex 5 μ m C₁₈ column (150 x 4.6 mm) using acetonitrile and H₂O with 0.1% formic acid as the two solvents in a linear gradient over 25 minutes at a flow rate of 0.7 mL/min. The top graph is the chromatogram of the sample while the middle is the MS¹ spectrum of the chromatogram peak at 18.53 minutes. The bottom spectrum is the MS² spectrum of the 817 m/z ion.

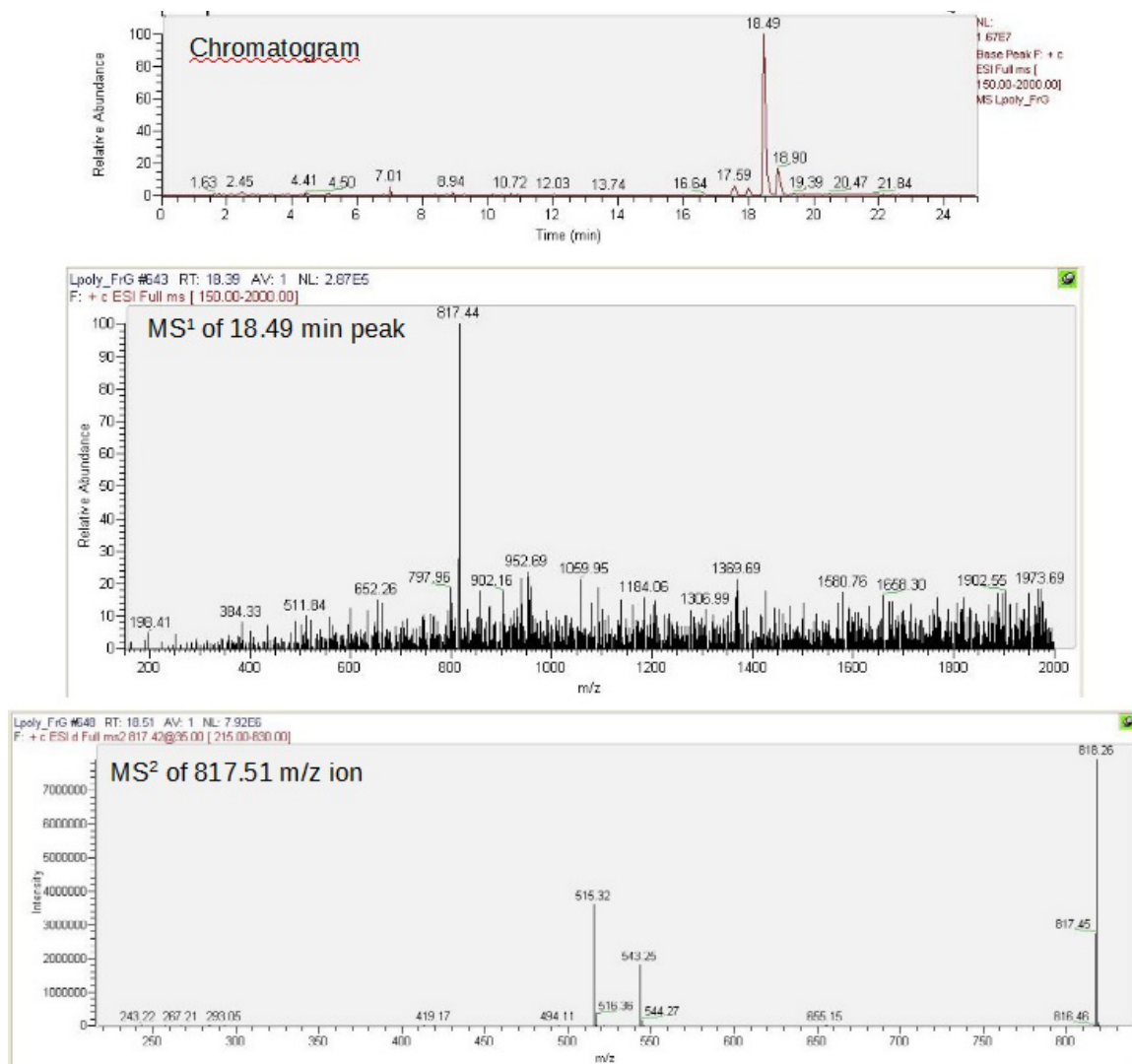


Figure 4.3. Liquid Chromatography-Mass Spectrometry Analysis of Fraction G. Liquid chromatography-mass spectrometry analysis was performed on Fraction G of the *L. polyedrum* cell extract. The analysis was performed on a Phenomenex Kinetex 5 μ m C₁₈ column (150 x 4.6 mm) using acetonitrile and H₂O with 0.1% formic acid as the two solvents in a linear gradient over 25 minutes at a flow rate of 0.7 mL/min. The top graph is the chromatogram of the sample while the middle is the MS¹ spectrum of the chromatogram peak at 18.49 minutes. The bottom spectrum is the MS² spectrum of the 817 m/z ion.

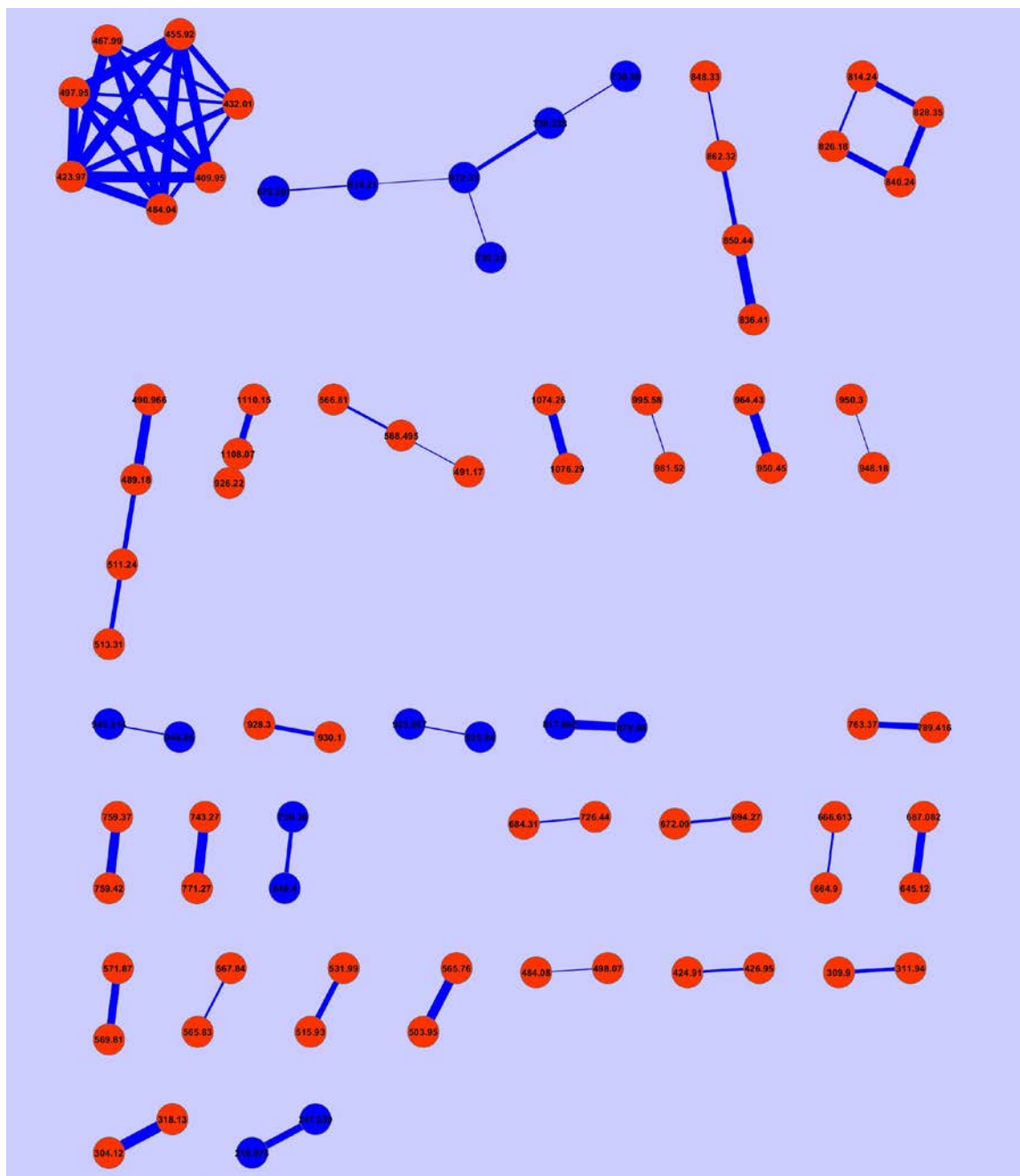


Figure 4.4. **Molecular Network of *L. polyedrum* Cell and Media Extract Fractions.**

This network was generated utilizing the molecular network platform provided by Global Natural Products Social Molecular Networking (GNPS). Blue nodes represent ions originating from *L. polyedrum* fractions, while orange nodes represent pure compounds from the Gerwick Lab pure compounds library. A minimum cosine score to match was set as 0.7 with a minimum number of matched peaks to match set as 4. This network was run with the GNPS provided compound libraries. The nodes are labeled as the m/z values of the parent ions.

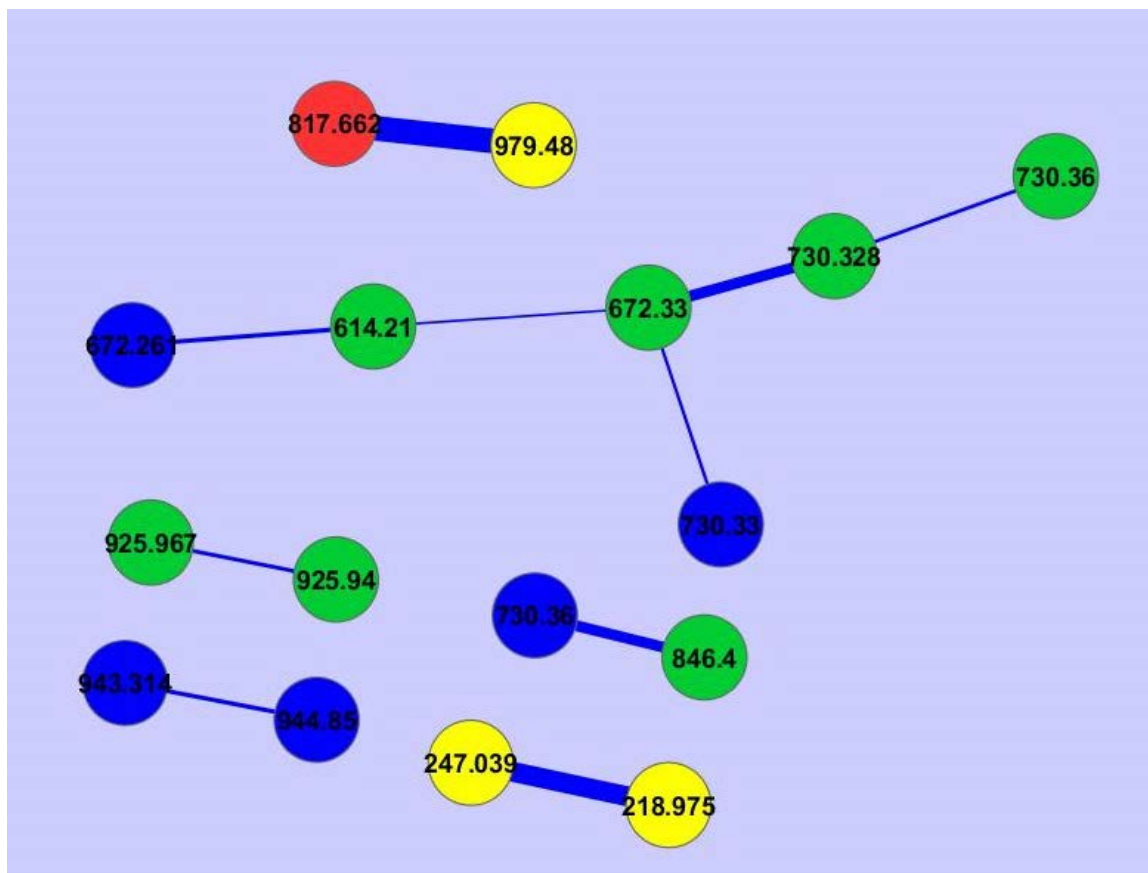


Figure 4.5. **Molecular Network of *L. polyedrum* Cell and Media Extract Fractions Excluding Library Ions.** This network was generated utilizing the molecular network platform provided by Global Natural Products Social Molecular Networking (GNPS). Red nodes represent molecules from Fraction F and G, yellow fractions represent molecules from Fractions E, green nodes represent molecules from media fraction M4, and blue nodes represent molecules from media fraction M5. A minimum cosine score to match was set as 0.7 with a minimum number of matched peaks to match set as 4. Single unmatched molecules were removed. This network was run with the GNPS provided compound libraries. The nodes are labeled as the m/z values of the parent ions.

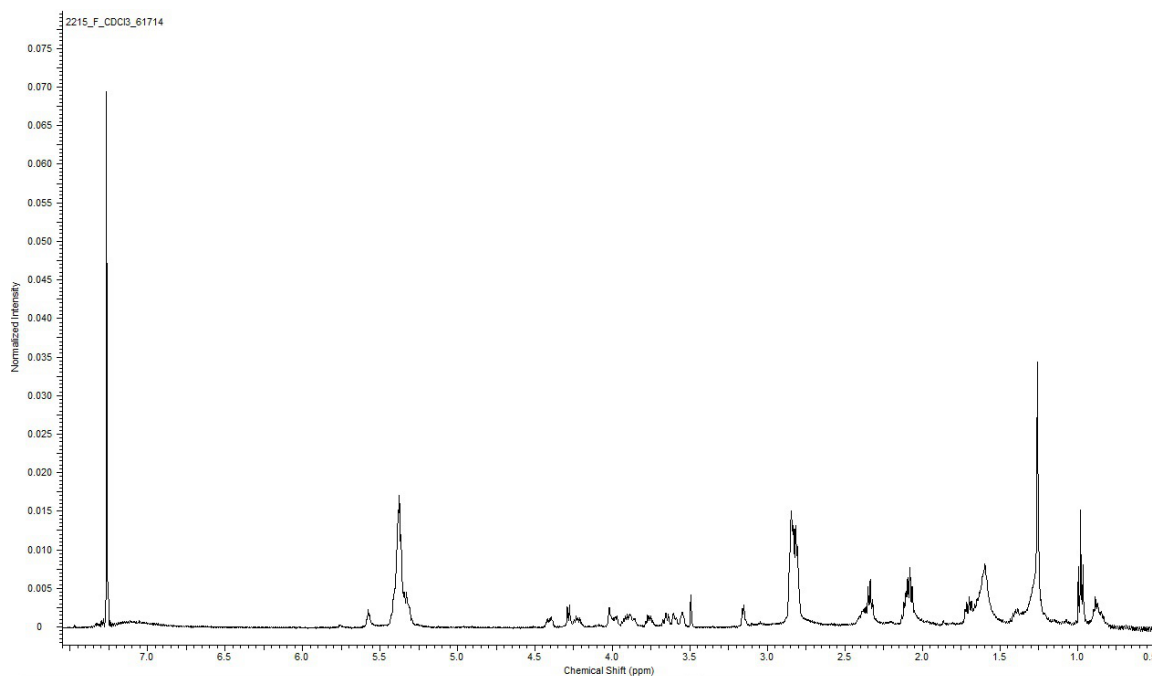
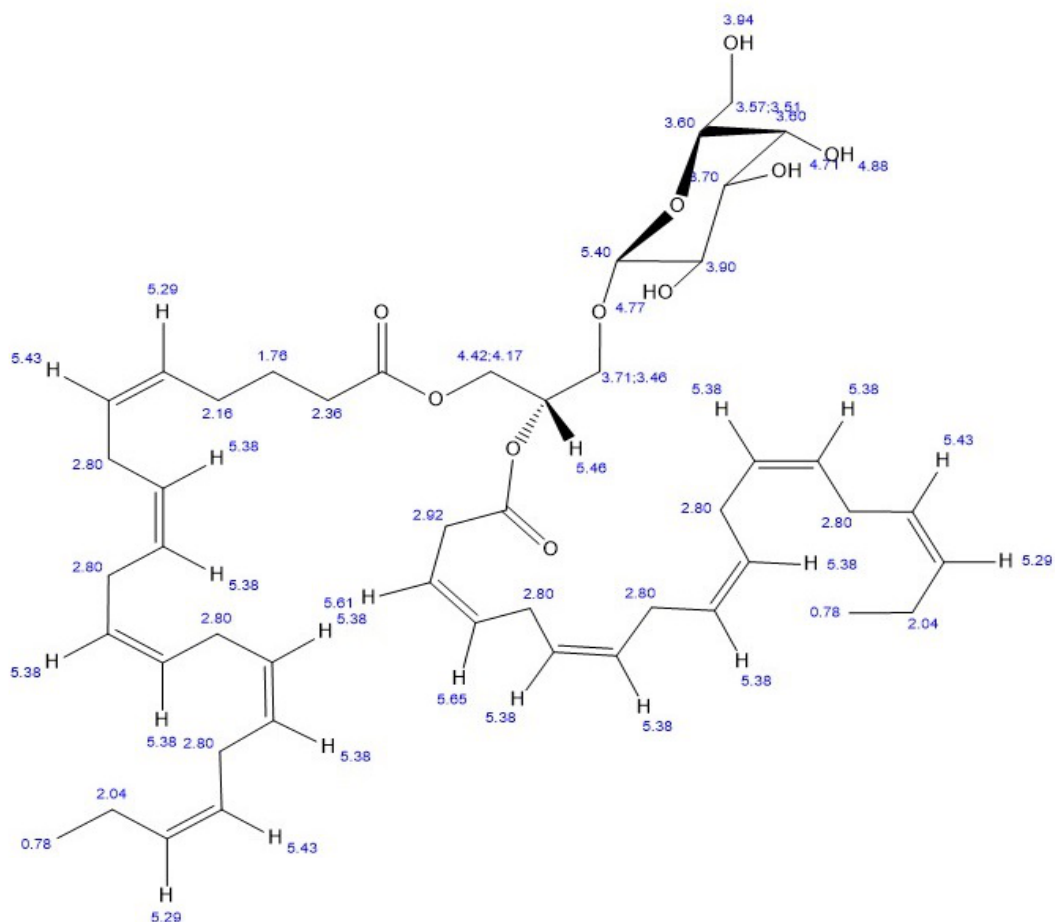


Figure 4.6. 1D Proton NMR Analysis of Fraction F. 1D proton NMR analysis of fraction F of *L. polyedrum* cell extract was performed. The fraction was dissolved in deuterated chloroform (CDCl_3) and sonicated to dissolve any particulates in the sample. A total of 64 scans were performed.

ChemNMR ^1H Estimation

Estimation quality is indicated by color: **good**, **medium**, **rough**

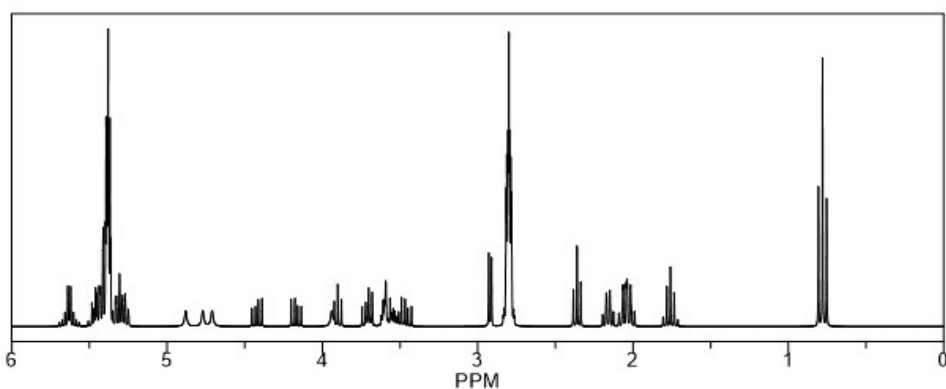


Figure 4.7. **1D Proton NMR Prediction of Proposed Monogalactosyldiacylglycerol (20:5/18:5) Structure.** A predicted 1D NMR spectrum of monogalactosyldiacylglycerol (20:5/18:5) was generated using ChemDraw. The numbers beside each proton location indicate the predicted peak shift (δ) in ppm.

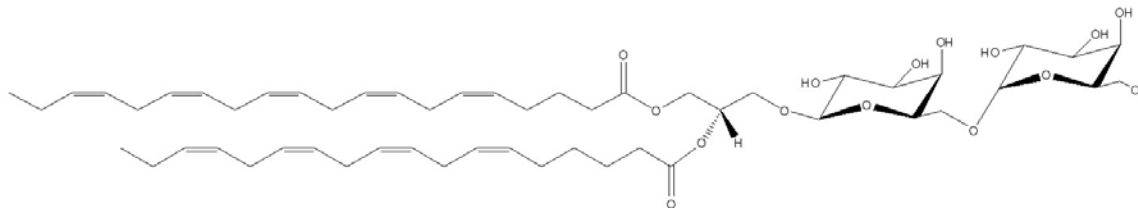


Figure 4.8. Chemical Structure of Digalactosyldiacylglycerol (20:5/18:5).
Digalactosyldiacylglycerol (20:5/18:5) was isolated from *L. polyedrum* cell fraction F.
This chemical structure was generated utilizing ChemDraw.

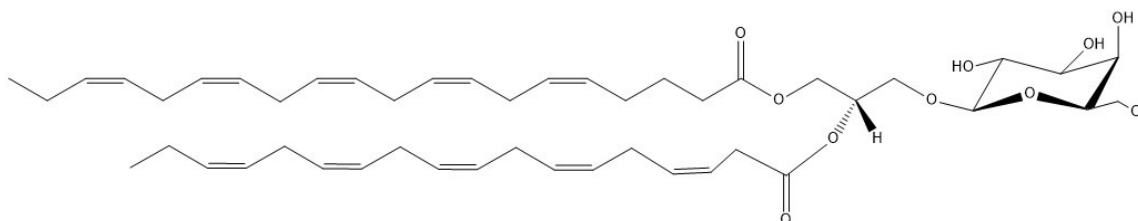


Figure 4.9. Chemical Structure of Monogalactosyldiacylglycerol (20:5/18:5).
Monogalactosyldiacylglycerol (20:5/18:5) was isolated from *L. polyedrum* cell fraction F.
This chemical structure was generated utilizing ChemDraw.

Nitric Oxide Production and Cytotoxicity of Digalactosyldiacylglycerol (20:5/18:5)

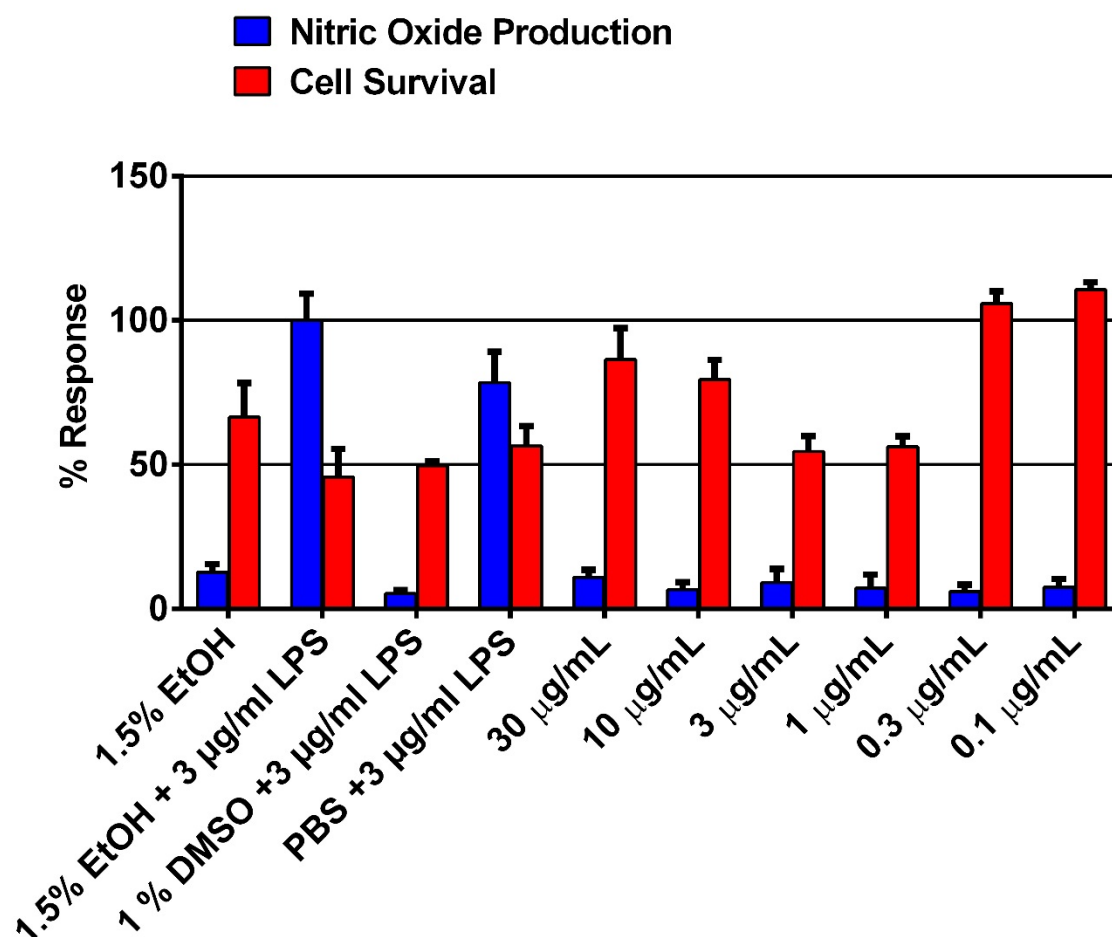


Figure 4.10. **Digalactosyldiacylglycerol (20:5/18:5) Inflammation and Cytotoxicity Assay.** Digalactosyldiacylglycerol (20:5/18:5) was isolated from *L. polyedrum* cell fraction F and dissolved in ethanol. DGDG (20:5/18:5) was then introduced to RAW264.7 murine macrophage cells at 30 µg/mL, 10 µg/mL, 3 µg/mL, 1 µg/mL, 0.3 µg/mL, and 0.1 µg/mL in triplicate and allowed to incubate for 24 hours before testing the cell media solution for nitric oxide concentration utilizing the Griess reagent reaction. The remaining RAW264.7 cells were then aspirated and tested in a cell proliferation assay utilizing MTT staining. The data shown utilizes the response of the positive control, 3 µg/mL LPS in 1.5% ethanol, as the base 100% response for nitric oxide production and cell survival.

Nitric Oxide Production and Cytotoxicity of Monogalactosyldiacylglycerol (20:5/18:5)

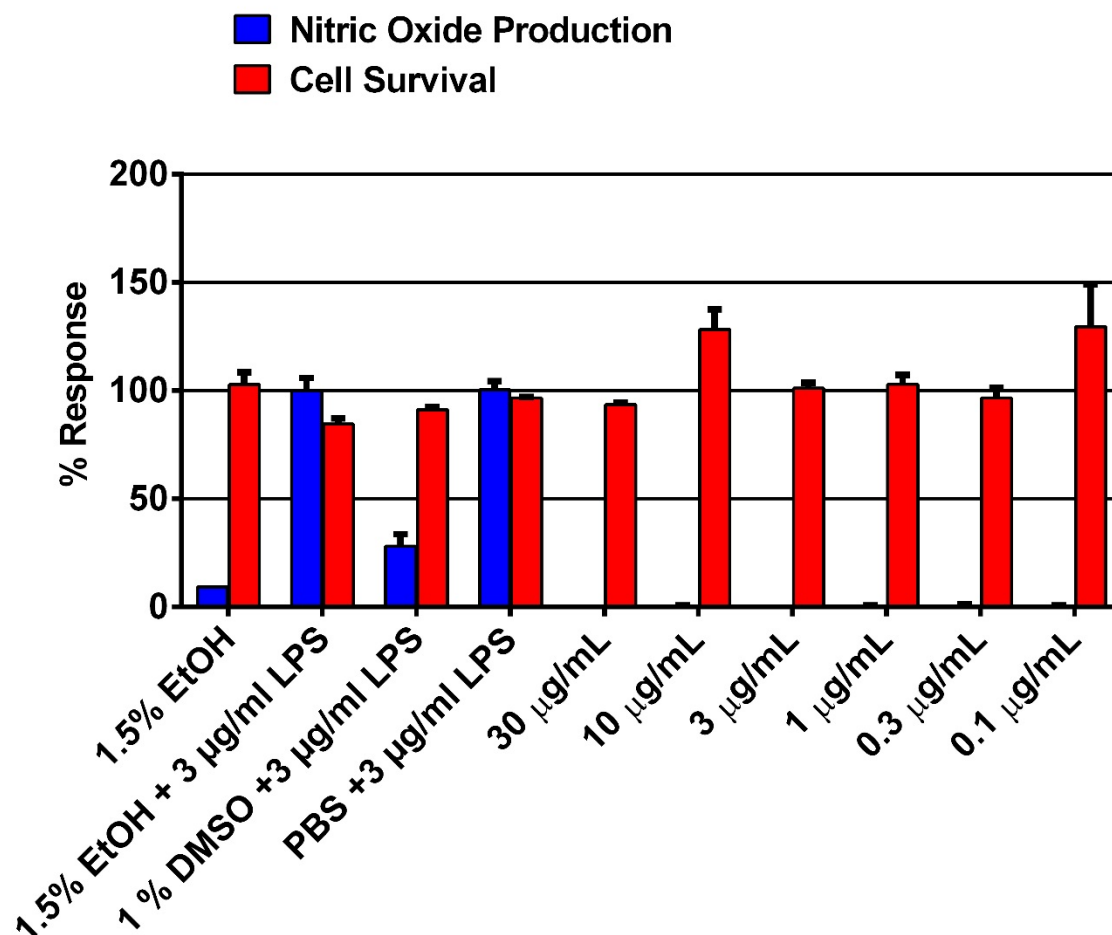


Figure 4.11. Monogalactosyldiacylglycerol (20:5/18:5) Inflammation and Cytotoxicity Assay. Monogalactosyldiacylglycerol (20:5/18:5) was isolated from *L. polyedrum* cell fraction F and dissolved in ethanol. DGDG (20:5/18:5) was then introduced to RAW264.7 murine macrophage cells at 30 µg/mL, 10 µg/mL, 3 µg/mL, 1 µg/mL, 0.3 µg/mL, and 0.1 µg/mL in triplicate and allowed to incubate for 24 hours before testing the cell media solution for nitric oxide concentration utilizing the Griess reagent reaction. The remaining RAW264.7 cells were then aspirated and tested in a cell proliferation assay utilizing MTT staining. The data shown utilizes the response of the positive control, 3 µg/mL LPS in 1.5% ethanol, as the base 100% response for nitric oxide production and cell survival.

Chapter Five

Extraction of *L. polyedrum* cell culture for Yessotoxin-like Metabolites

5.1. Yessotoxin-like Metabolite Extraction of *L. polyedrum* Cell Cultures

From previous work done in the Gerwick group by Alban Pereira, yessotoxin-like metabolites of similar mass to yessotoxin were found upon extraction of *L. polyedrum* bloom samples and LCMS analysis. The samples were extracted with a method different from the method initially used to extract the *L. polyedrum* cells. Cells were separated from media through vacuum filtration as previously done, however the cells were instead dissolved in 100% methanol. This methanol extract was dried on rotary evaporator and then partitioned between 200 mL of hexanes and 200 mL of 4:1 methanol:water in a 500 mL separatory funnel. The methanolic layer was separated and suspended in water before being extracted in butanol. The butanol layer was then dried down on rotary evaporator to obtain a mass of 332.2 mg. It was this layer which was previously reported to have yessotoxin-like metabolites.

Yessotoxin was purchased and analyzed on LCMS as a chemical standard to compare with *L. polyedrum* extracts. The yessotoxin standard was dissolved in methanol and run on the LCMS in negative mode. The solvents used were acetonitrile, solvent A, and water, solvent B. The flow was first a constant flow of 5% solvent A and 95% solvent B for 5 minutes which was followed by a linear gradient to 95% solvent A and 5% solvent B over 10 minutes which was then held for 5 minutes. This hold was then followed by a linear gradient back to initial solvent conditions of 5% solvent A and 95% solvent B over 1 minute which is held for another 4 minutes. A total of 1 ug of standard was injected and the results of the analysis of this standard can be seen in Figure 5.. The initial *L. polyedrum* cell extractions as well as the yessotoxin-like metabolite extractions were run in the same LCMS conditions and compared to the yessotoxin standard,

however, no fractions contained observable amounts of yessotoxin. The cell fractions were also analyzed for ions which were in the range of yessotoxin analogs, specifically between the range of 955-1551 amu, however no fractions contained peaks within this range or even significant peaks in negative mode (Paz,B et al 2008).

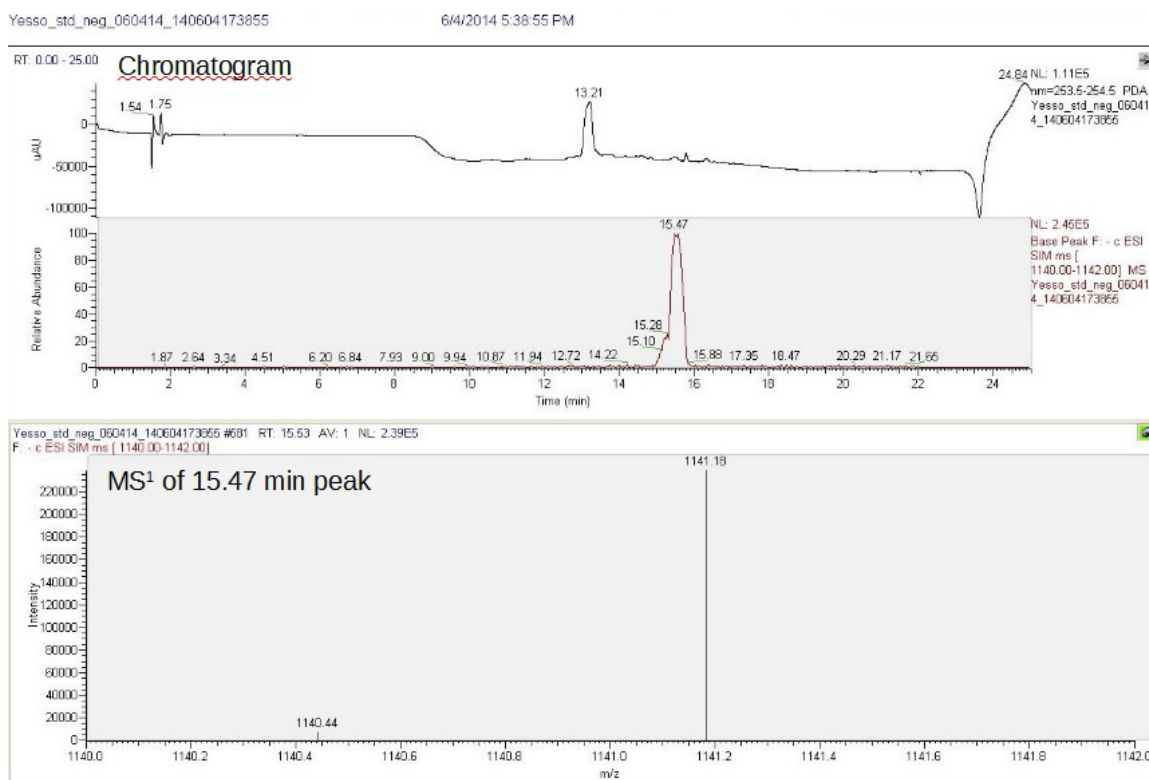


Figure 5.1. Liquid Chromatography-Mass Spectrometry Analysis of Yessotoxin Standard. Liquid chromatography-mass spectrometry analysis was performed on a sample of yessotoxin. The analysis was performed using a Phenomenex Kinetex 5 μm C₁₈ column (150 x 4.6 mm) using acetonitrile and H₂O as the two solvents in a linear gradient over 25 minutes at a flow rate of 0.7 mL/min. The top graph is the chromatogram of the sample while the bottom is the MS¹ spectrum of the chromatogram peak at 15.47 minutes.

Chapter Six
Discussion and Conclusions

6.1 Discussion

The inactivity of the isolated glycolipids MGDG (20:5/18:5) and DGDG (20:5/18:5) is perplexing as these glycolipids are the major components of the most active *L. polyedrum* cell fractions. This raises more questions regarding the cause of the inflammatory response elicited by the RAW264.7 cells. It is not impossible that these glycolipids could be bioactive compounds as many glycolipids have previously been shown to be very bioactive. As an example, invariant natural killer T cells (NKT cells) have been shown to recognize diacylglycerol-containing glycolipids when presented by CD1d proteins, inducing the production of cytokines to elicit an inflammatory response (Kinjo, Y 2011). Similarly, monogalactosyl monoacylglycerol and two digalactosyl monoacylglycerols were isolated from a different dinoflagellate species, *Heterocapsa circularisquama*, and were shown to cause cytolytic activity in the heart and gills of oysters (Hiraga, Y. 2007).

The inactivity of the glycolipids in isolation may be due to a number of possibilities. The glycolipids may work synergistically with another compound in the cell fraction to induce a pro-inflammatory response. It may also be that there simply is a separate active compound found in the same fraction which may have been overlooked, or present in such low quantity that it was not detectable during LCMS analysis. Alternatively, the active compound may have simply been lost or decomposed in the process of chemical analysis. Another assay of *L. polyedrum* cell extract fractions should be undertaken to confirm the pro-inflammatory activity. The use of a different cell line and assay may also be helpful in confirming pro-inflammatory activity.

One possibility would be the use of HMC-1 human mast cells and measuring the expression of pro-inflammatory cytokines after exposure (Park, H. et al 2007). HMC-1 human mast cells would be a better indicator of allergic response as mast cells are key mediators in inflammatory and allergic response through inducing cytokine expression. This is key as many individuals had described their exposure to *L. polyedrum* blooms as similar to an allergic response.

Another cell line to be considered would be Natural Killer T cells (NKT cells). Previous work has shown NKT cells initiating an immune response, releasing IFN- γ and IL-4, upon exposure to glycolipids. A specific strain of NKT cells, V α 14 iNKT, recognizes specifically diacylglycerol containing glycolipids when these glycolipids are presented by the CD1d protein (Kinjo, Y. 2011). As both glycolipids isolated in this work both contain diacylglycerol, testing with these cells may be worth investigating.

There were also other molecules present in both fractions F and G which may be worth further investigation. A chromatograph peak at 17.59 minutes present in both F and G fractions share a 789.42 m/z ion which fragments similarly for both, as shown in figure 6.1. Analysis of the difference in mass between the parent ion and a 515 m/z ion shows a 274 mass loss which is similar in mass to the cleavage of the 18:5 fatty acid chain seen in both MGDG(20:5/18:5) and DGDG(20:5/18:5). As no other fragmented ion mass were detected, it is predicted that this 789.42 m/z ion is a similar MGDG glycolipid with two 18:5 fatty acid chains, as proposed in figure 6.2. Another peak at 18.90 minutes also present in both fractions reveals an 819 m/z ion which fragments similarly to MGDG(20:5/18:5) as seen in figure 6.3. Comparing MGDG(20:5/18:5) and this 819 m/z reveals a mass difference of 2 and comparing the MS² fragmentation of the two ions, the

difference in fragmentation is a 517 m/z ion compared to the 515 m/z ion present in the fragmentation of MGDG(20:5/18:5). This ion is a result of the cleavage of the 20:5 fatty acid chain, indicating there is a difference in the mass of the 18 carbon chain in comparing the two. This would be easily explained by the 18 carbon chain in this 819 m/z ion having one less unsaturation, resulting in MGDG(20:5/18:4) which is proposed in figure 6.4. As F and G were the most potent fractions tested and the glycolipids isolated were not active, one of the next steps in this work would be to isolate ions which are common to both fractions and determine whether these possible glycolipids had caused the observed activity.

While *L. polyedrum* is a known producer of yessotoxin, there was no detectable trace of yessotoxin or yessotoxin analogues found in the LCMS analysis of cell extraction fractions when comparing the extracts to a yessotoxin standard. This may be due to differences in gene expression between the cultured *L. polyedrum* which was used here and the *L. polyedrum* environmental samples collected directly from the algal bloom. This would not be unprecedented as other *L. polyedrum* species have been found that do not produce yessotoxin (Moorthi, SD et al 2006).

Another avenue of further inquiry lies in the inflammatory response experienced by the researchers involved in the handling of *L. polyedrum* cultures. During the process of transferring the *L. polyedrum* cultures, the researchers handling the cultures experienced some respiratory issues as well as lightheadedness, although not all members of the lab had the same reaction to the cultures. It is possible that there is an active molecule which may be found in the headspace of the culture or possibly is aerosolized from the media. A headspace analysis of the *L. polyedrum* culture may lead to the

discovery of an active compound. In a broader scope, it may be worthwhile to gather individuals who respond to exposure to the cell culture and determine commonalities between these affected individuals through genetic analysis.

6.2. Conclusions

While the cell extract fractions of *L. polyedrum* exhibited inflammatory response as well as cytotoxic activity, isolation and testing of the major molecule found in the most active fractions, MGDG (20:5/18:5), was found to be inactive as both a pro-inflammatory agent and as a cytotoxic molecule, as is the similar glycolipid DGDG (20:5/18:5). This suggests that neither of these glycolipids are pro-inflammatory or cytotoxic in nature, at least not in their isolated state. Yessotoxin is also unlikely to be the active molecule in this dinoflagellate as no yessotoxin or yessotoxin-like metabolites were found within cell extracts at detectable concentrations.

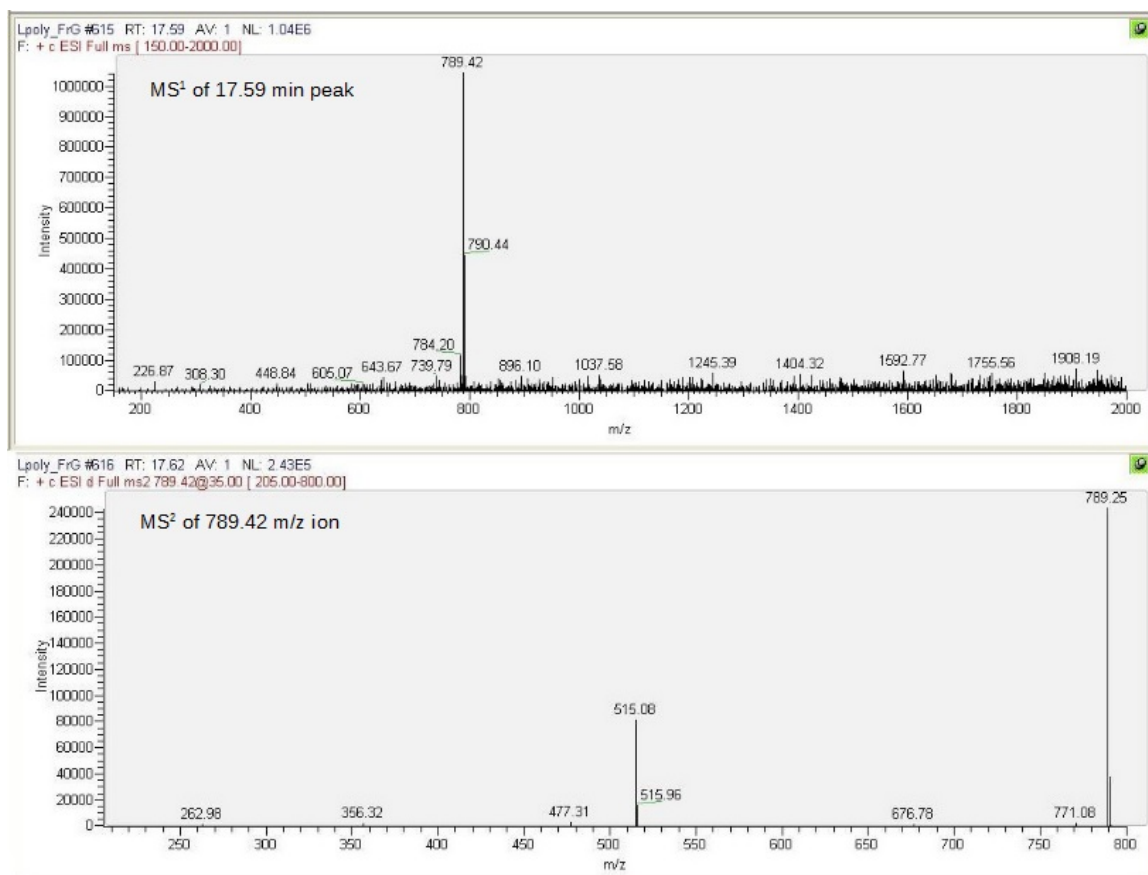


Figure 6.1. Liquid Chromatography-Mass Spectrometry Analysis of 17.59 minute peak in Fraction G. Liquid chromatography-mass spectrometry analysis was performed on Fraction G of the *L. polyedrum* cell extract. The analysis was performed on a Phenomenex Kinetex 5 μm C₁₈ column (150 x 4.6 mm) using acetonitrile and H₂O with 0.1% formic acid as the two solvents in a linear gradient over 25 minutes at a flow rate of 0.7 mL/min. The top graph is the MS¹ spectrum of the chromatogram peak at 17.59 minutes. The bottom spectrum is the MS² spectrum of the 789.42 m/z ion.

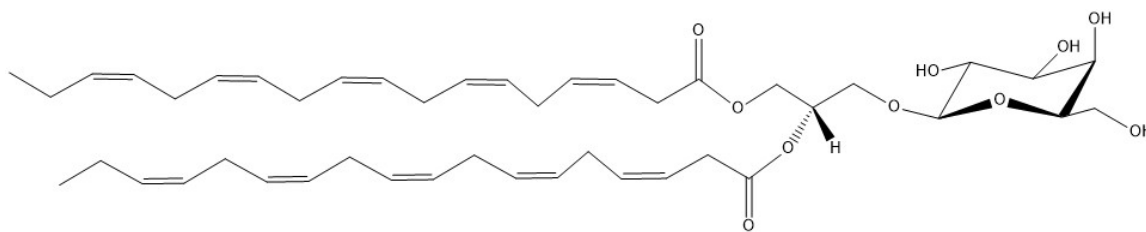


Figure 6.2. Chemical Structure of Monogalactosyldiaclyglycerol (18:5/18:5). Suggested structure of 789.42 m/z ion found in *L. polyedrum* cell fractions F and G. This chemical structure was generated utilizing ChemDraw.

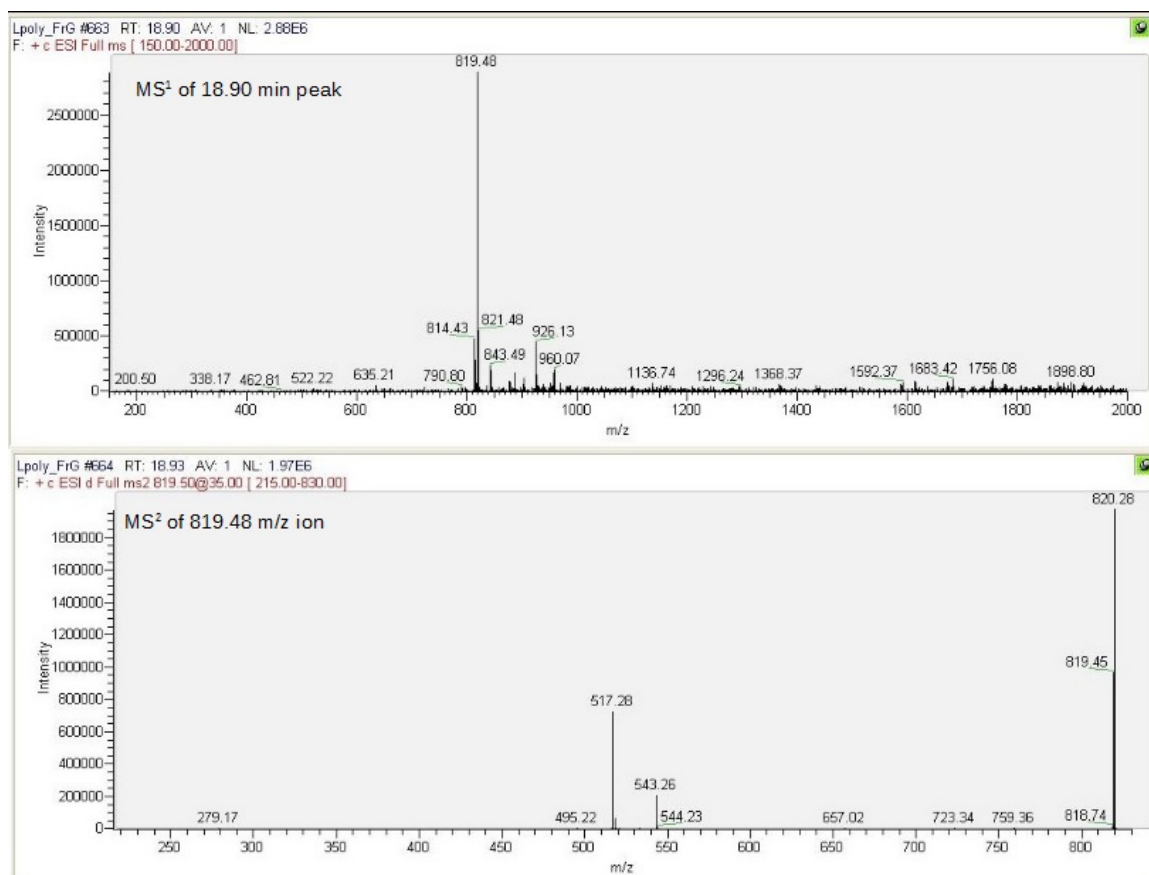


Figure 6.3. Liquid Chromatography-Mass Spectrometry Analysis of 18.90 minute peak in Fraction G. Liquid chromatography-mass spectrometry analysis was performed on Fraction G of the *L. polyedrum* cell extract. The analysis was performed on a Phenomenex Kinetex 5 μm C₁₈ column (150 x 4.6 mm) using acetonitrile and H₂O with 0.1% formic acid as the two solvents in a linear gradient over 25 minutes at a flow rate of 0.7 mL/min. The top graph is the MS¹ spectrum of the chromatogram peak at 18.90 minutes. The bottom spectrum is the MS² spectrum of the 819.48 m/z ion.

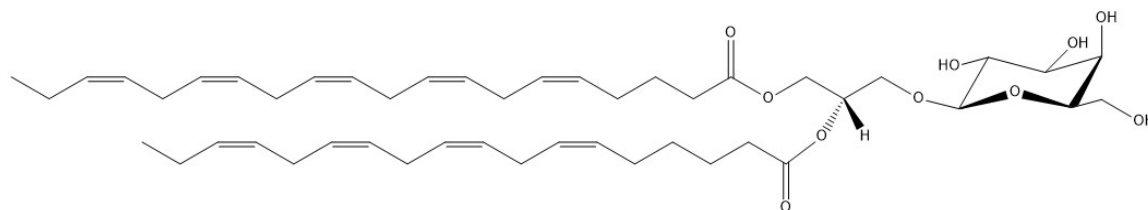


Figure 6.4. Chemical Structure of Monogalactosyldiaclyglycerol (20:5/18:4). Suggested structure of 819.48 m/z ion found in *L. polyedrum* cell fractions F and G. This chemical structure was generated utilizing ChemDraw.

References

- Allen, W.E. (1946). "BRed water in La Jolla Bay in 1945." Trans Am Microsc Soc **65**: 262–264
- Anderson, D.M., Burkholder, J.M., Cochlan, W., Glibert, P.M., Cobler, C.J., Heil, C.A., Kudela, R.M., Parsons, M.L., Rensel, J.E., Townsend, D.W., Trainer, V.L., Vargo, G.A. (2008). "Harmful algal blooms and eutrophication: examining linkages from selected coastal regions of the United States." Harmful Algae **8**(1):39–53
- Antonopoulou, S., Nomikos, T., Oikonomou, A., Kyriacou, A., Andriotis, M., Fragopoulou, E., Pantazidou, A. (2005). "Characterization of bioactive glycolipids from *Scytonema julianum* (cyanobacteria)." Comparative Biochemistry and Physiology **140**:219-231
- Bell, G.R. (1961). "Penetration of spines from a marine diatom into gill tissue of Lingcod (*Ophiodon elongatus*)." Nature **192**(479):279–280
- Ciglonecki, I. (2003). "Mucopolysaccharide transformation by sulfide in diatom cultures and natural mucilage." Mar Ecol Prog Ser **263**:17–27
- Croxall, J.P., Nicol, S. (2004). "Management of southern ocean fisheries: global forces and future sustainability." Antarct Sci **16**(4):559–584
- Dagg, M.J. (2007). "A review of water column processes influencing hypoxia in the northern Gulf of Mexico." Estuaries Coast **30**(5):735–752

Franchini, A., Marchesini, E., Poletti, R., Ottaviani, E. (2004). "Lethal and sub-lethal yessotoxin dose-induced morpho-functional alterations in intraperitoneal injected Swiss CD1 mice." Toxicon **44**: 83-90.

Franchini, A., Marchesini, E., Poletti, R., Ottaviani, E. (2004). "Acute toxic effect of the algal yessotoxin on Purkinje cells from cerebellum of Swiss CD1 mice." Toxicon **43**: 347-352.

Gray, C.G., Lasiter, A.D., Li, C., Leblond, J.D. (2009). "Mono- and digalactosyldiacylglycerol composition of dinoflagellates. I. Peridinin-containing taxa." European Journal of Phycology **44**:2, 191-197

Hallegraeff, G.M. (1993). "A review of harmful algal blooms and their apparent global increase." Phycologia **32**:79-99

Hallegraeff, G.M. (2010). "Ocean climate change, phytoplankton community responses, and harmful algal blooms: a formidable predictive challenge." J Phycol **46**(2):220-235

Hastings, J.W. (2007). "The Gonyaulax clock at 50: translational control of circadian expression." Cold Spring Harb Symp Quant Biol **72**: 141-144.

Heisler, J., Glibert, P.M., Burkholder, J.M., Anderson, D.M., Cochlan, W., Dennison, W.C., Dortch, Q., Cobler, C.J., Heil, C.A., Humphries, E., Lewitus, A., Magnien, R., Marshall, H.G., Sellner, K., Stockwell, D.A., Stoecker, D.K., Suddleson, M. (2008). "Eutrophication and harmful algal blooms: a scientific consensus." Harmful Algae **8**(1):3-13

Hiraga, Y., Shikano, T., Widiyanti, T., Ohkata, K. (2007). "Three new glycolipids with cytolytic activity from cultured marine dinoflagellate *Heterocapsa circularisquama*." Natural Product Research **22**(8):649-657

Holmes, R.W., Williams, P.M., Eppley, R.W. (1967). "Red water in La Jolla Bay, 1964–1966." Limnol Oceanogr **12**: 503–512

Huisman, J.M., Saunders, G.W. (2007). "Phylogeny and classification of the algae." Algae of Australia: introduction. Australian Biological Resources Study/CSIRO, Melbourne, pp 66–103

Kahru, M., Mitchell, B.G. (1998). "Spectral reflectance and absorption of a massive red tide off Southern California." J Geophys Res Oceans **103**: 21601–21609

Kent, M.L., Whyte, J.N.C., Latrace, C. (1995). "Gill lesions and mortality in seawater pen-reared Atlantic salmon *Salmo-Salar* associated with dense bloom of *Skeletonema costatum* and *Thalassiora* species." Dis Aquat Organ **22**(1):77–81

Kinjo, Y. (2011). "Invariant natural killer T cells recognize glycolipids from pathogenic Gram-positive bacteria." Nature Immunology **14**:10, 966-975

Kubanek, J. (2005). "Does the red tide dinoflagellate *Karenia brevis* use allelopathy to outcompete other phytoplankton?" Limnol Oceanogr **50**(3):883–895

Kudela, R.M., Cochlan, W.P. (2000). "Nitrogen and carbon uptake kinetics and the influence of irradiance for a red tide bloom off southern California." Aquatic Microbial Ecology **21**: 31–47.

Lancelot, C. (2011). "Cost assessment and ecological effectiveness of nutrient reduction options for mitigating *Phaeocystis* colony blooms in the southern North Sea: an integrated modeling approach." Sci Total Environ **409**(11):2179–2191

Laws, R.M. (1985). "The ecology of the southern ocean." Am Sci **73**(1):26–40

Legrand, C. (2003). "Allelopathy in phytoplankton – biochemical, ecological, and evolutionary aspects." Phycologia **42**:406–419

Malaguti, C., Ciminiello, P., Fattorusso, E., Rossini, G.P. (2002). "Caspase activation and death induced by yessotoxin in HeLa cells." Toxicology in Vitro **16**:357-363.

McLean, T.I., Sinclair, G.A. (2012). "Harmful Algal Blooms. Environmental Toxicology" Springer, New York, pp 319-360

Moorthi, S.D., Countway, P.D., Stauffer, B.A., Caron, D.A. (2006). "Use of quantitative real-time PCR to investigate the dynamics of the red tide dinoflagellate *Lingulodinium polyedrum*." Microb Ecol **52**: 136–150.

Okaichi, T., Nishio, S. (1976). "Identification of ammonia as the toxic principle of red tide of *Noctiluca miliaris*." Bull Plankton Soc Jpn **23**:75–80

Park, H., Lee, S., Oh, J., Lee, M., Yoon, K., Park, B.H., Kim, J.W., Song, H., Kim, S. (2007). "Anti-inflammatory activity of fisetin in human mast cells (HMC-1)." Pharmacological Reserach **22**(1):31-37

Paz, B., Daranas, A.H., Norte, M., Riobo, P., Franco, J.M., Fernandez, J.J. (2008). "Yessotoxins, a Group of Marine Polyether Toxins: an Overview." Marine Drugs **6**:73-102

Rabalais, N.N. (2002). "Nutrient-enhanced productivity in the northern Gulf of Mexico: past, present and future." Hydrobiologia **475**(1):39–63

Smayda, T.J., White, A.W. (1990). "Has there been a global expansion of algal blooms? If so is there a connection with human activities?" Toxic marine phytoplankton Elsevier, New York, pp 516–517

Smayda, T.J. (1990). "Novel and nuisance phytoplankton blooms in the sea: evidence for a global epidemic." Toxic marine phytoplankton Elsevier, New York, pp 29–40

Smayda, T.J. (1992). "Global epidemic of noxious phytoplankton blooms in the sea: evidence for a global epidemic." Food chains: models and management of large marine ecosystems Westview Press, San Francisco, pp 275–307

Smayda, T.J., Reynolds, C.S. (2001). "Community assembly in marine phytoplankton: application of recent models to harmful dinoflagellate blooms." J Plankton Res **23**(5):447–461

Smayda, T.J., Reynolds, C.S. (2003). "Strategies of marine dinoflagellate survival and some rules of assembly." J Sea Res **49**(2):95–106

Sournia, A. (1974). "Circadian periodicities in natural populations of marine phytoplankton." Mar Biol **12**:325–389

Torrey, H.B. (1902). "An unusual occurrence of dinoflagellata on the California coast." Am Nat **36**: 187–192

Vargo, G.A. (2001). "The hydrographic regime, nutrient requirements, and transport of a *Gymnodinium breve* Davis red tide on the west Florida shelf." Harmful algal blooms 2000. Intergovernmental Oceanographic Commission of UNESCO, Paris, pp 157–159